REGIONAL HAZARD AND LOSS MODELING FOR FLOODS AND DEBRIS FLOWS

A Thesis

by

Fidence Cyizere Rukundo

Submitted to the

Graduate School of Sciences and Engineering

In Partial Fulfillment of the Requirements for

the Degree of

Master of Science

in the

Department of Civil Engineering

Özyeğin University

September 2023

REGIONAL HAZARD AND LOSS MODELING FOR FLOOD AND DEBRIS FLOW

Advisor: Asst. Prof. Derya Deniz

Co-Advisor: Asst. Prof. Yiğit Can Altan

Approved by:

Asst. Prof. Derya Deniz, Advisor,
Department of Civil Engineering
Özyeğin University

Asst. Prof. Senem Seyis
Department of Civil Engineering
Özyeğin University

Prof. Cevza Melek Kazezyılmaz Alhan, Department of Civil Engineering
Istanbul University-Cerrahpaşa

Date Approved: 27 July 2023

ABSTRACT

Natural hazards pose threats to built environments and society at large. Given their sheer effects, it is imperative that researchers redirect their efforts to better understand and anticipate their havoc before they come. This study addresses two of the most prevalent rainfall-triggered natural disasters, namely, flooding and debris flow. A flood hazard analysis for the town of Bozkurt in Turkiye is performed using the August 11th, 2021, flood data. Similarly, a debris flow analysis for the town of Sarno in Italy is performed using the May 5th, 1998, Sarno debris flow data. Then, using the building information data in the studied areas, exposure analyses are performed in a Geographic Information System (GIS) program for both the flood and debris flow events. To estimate the individual building's losses, different damage curves and formulations in the literature are used and the total buildings losses are calculated. Knowing that hazard modeling and loss estimations involve so many uncertainties, the study seeks to investigate the effects of uncertainties on the overall regional hazard costs for both the flood and debris flow events. Sensitivity analyses are then performed to investigate the relationship between the flood discharge to the regional losses in the town of Bozkurt and the debris flow volume to the regional losses in the town of Sarno. For the regional hazard loss estimates for Bozkurt and Sarno, the models that include both uncertainties and spatial correlations are considered. It is concluded that there is a strong relationship between flood flow rate and regional losses for the town of Bozkurt and it can be inferred that there exist flood discharge-regional loss relationships for other flood prone towns in Turkiye as well. Similarly, results on the town of Sarno, Italy show that there exists a relationship between debris flow volume and regional loss.

ÖZETÇE

Doğal afetler, yapılı çevre ve toplum için ciddi tehdit oluşturmaktadır. Afetlerin etkileri göz önüne alındığında, araştırmacıların çabalarını afetlerin gelmeden önce yıkıcı etkilerini daha iyi anlamak ve öngörmek için yönlendirmesi önemlidir. Bu çalışma, en yaygın olarak görülen yağışla tetiklenen doğal afetlerden ikisi olan taşkın ve debris (moloz) akışı ile ilgilenmektedir. Çalışmada Türkiye'nin Bozkurt ilçesi için 11 Ağustos 2021 taşkın verileri kullanılarak bir sel tehlikesi analizi ve 5 Mayıs 1998 tarihli Sarno heyelan verileri kullanılarak İtalya'daki Sarno bölgesi için bir debris akışı analizi gerçekleştirilmiştir. Sonrasında, çalışılan bölgeye ait bina verileri kullanılarak, bir Coğrafi Bilgi Sistemleri (GIS) programında hem taşkın hem de çamur-moloz akışı için etki analizleri gerçekleştirilmiştir. Bireysel bina kayıplarını tahmin etmek için literatürdeki olan çeşitli hasar eğrileri ve formülasyonları kullanılmış ve buradan toplam bina kayıpları hesaplanmıştır. Tehlike modellemesinin ve kayıp tahminlerinin çok sayıda belirsizlik içerdiği göz önünde bulundurularak, bu çalışmada hem taşkın hem de debris akışı için toplam bölgesel tehlike maliyetleri üzerindeki belirsizliklerin etkileri araştırılmaya çalışılmıştır. Daha sonra, Bozkurt ilçesindeki taşkın debisi ve Sarno ilçesindeki debris akışı hacmi ile bölgesel kayıplar arasındaki ilişkiyi araştırmak için duyarlılık analizleri yapılmıştır. Bozkurt ilçesindeki taşkın olayları için, belirsizlikleri ve mekansal korelasyonları dikkate alan taşkın tehlike kayıpları tahmin modelleri kullanılmıştır. Benzer şekilde, Bozkurt ilçesindeki taşkın debisi ve Sarno bölgesindeki debris akış hacmi ile bölgesel kayıplar arasındaki ilişkiyi araştırmak için duyarlılık analizleri yapılmıştır. Bozkurt ilçesindeki taşkın olayları için, belirsizlikleri ve mekânsal korelasyonları dikkate alan taşkın tehlikesi kaybı tahmin modelleri önerilmektedir. Bozkurt ilçesi için taşkın debi ile bölgesel finansal kayıplar arasında güçlü bir ilişki

olduğu sonucuna varılmıştır ve Türkiye'deki diğer taşkın eğilimli kasabalar için de taşkın debi-bölgesel kayıp ilişkilerinin var olduğu çıkarılabilmektedir. Benzer şekilde, Sarno, İtalya'daki bölge üzerinde bir taşkın akıntısı duyarlılık analizi de gerçekleştirilmiş ve debris akış hacmi ile bölgesel kayıp arasında bir ilişkinin var olduğu önerilmiştir.

ACKNOWLEDGMENTS

"If I have seen further, it is by standing on the shoulders of the giants."

-Isaac Newton-

First and foremost, I would like to thank God for his grace and unfailing love that has carried me through all this long but fulfilling journey.

This work is a result of not only my two years in masters, but of all the steps that took me to this point. I would therefore like to express my deepest gratitude to whomever contributed to my education so far, be it financial support, advice, encouragement, learning and guidance. I specifically want to express my deepest gratitude to my advisor Dr. Derya Deniz who has guided and assisted me in my master's education and research. I equally thank my co-advisor Dr. Yiğit Can Altan for all the advice and assistance during my research.

Finally, I would like to thank Özyeğin University for the financial support throughout my master's program and the government of Turkey during my undergraduate education. I also owe so much to my family, especially my mother for the sacrifices she has made.

TABLE OF CONTENTS

LIST OF TABLES

LIST OF FIGURES

CHAPTER I

INTRODUCTION

Natural hazards pose threats to build environments and society at large. Throughout history of humankind, people have tried to harness the forces of nature and reduce their catastrophic effects. Although there are tremendous and thus rewarding efforts and developments in the understanding of natural hazards, the problem has never been so alarming as it is today. Every day, the world faces escalating natural catastrophes due to unprecedented population growth, urbanization, and global climate change. The understanding and development in this field have always been hampered by some pressing issues like the presence of so many uncertainties, correct estimates of financial losses, quantification of non-monetary losses under limited availability of data, hazards complex interactions and their cascading effects. This study seeks to address two of the most prevalent rainfall-triggered natural disasters, namely, flooding and debris flow and to provide frameworks of hazard and loss assessments of each hazard separately.

To begin with, flooding is a rainfall triggered natural disaster that wreaks havoc to civil engineering structures. According to WHO (World Health Organization), more than 2 billion people were affected by floods for a period of fewer than 20 years (1998-2017). According to [1], the global economic losses due to flooding are estimated to be more than one trillion dollars between 1980 and 2013. Turkey, particularly, has suffered several flooding events in the last few decades, and their consequences are so rampant, second only to earthquake [2]. Additionally, although there have been so many studies on flood hazard modelling, little attention has been given to quantification of flood hazard economic losses. For this reason, this study intends to provide an all-inclusive procedure

that estimates community flood loss. Moreover, we try to include the effects of spatial correlation and uncertainties to understand their effect on the overall total economic hazard loss. August 11, 2021, Bozkurt flooding event is used as a case study for our work.

On August 11th, 2021, Bozkurt, among other Black Sea Regions of Turkey, experienced an unprecedented deadly flood following a two-days torrential rainfall [3]. Its consequences have been exacerbated by the presence of buildings in the floodplain, lack of proper flood mitigation measures, inadequate foundation depth, etc. This event has been chosen as our case study as it among the latest floods and it clearly represents well a typical flooding event in Turkey. Moreover, we intend to extend the research conducted on the Bozkurt, August 2021 flood and quantify its financial losses.

Another rainfall-induced natural hazard considered in this study is debris flow. Debris flow is among the types of landslides that affect mountainous regions. Landslides are one of the most disastrous natural hazards. They can cause significant damage to infrastructure, the economy, and society at large. According to the Global Landslide Catalog [4], there were over 11,000 fatal landslides worldwide between 2004 and 2016 resulting in the deaths of over 56,000 people. Globally, there have been over 1.6 million deaths and around $260-310 billion of economic loss every year since 1990 [5]. The estimated economic losses from those landslides were approximately $10 billion per year worldwide between 2004 and 2016. Turkey has also suffered a spate of rainfall-induced landslides that such as 2009 and 2010 Feke (in Adana) landslides, and 2010 Gündoğdu (Rize) landslides. As stated by [6], there are more than 45475 active landslides countrywide, mostly found in the Black Sea regions. As stated by [7], those landslides were mainly due to increased annual rainfall, limited availability of land due to population

growth which encourages people to construct buildings on steep places [8]. According to [9], landslides had led to more than 76995 building damages between 1959 and 1994 (35 years). According to [10], Turkey has suffered more than 1343 fatalities from more than 389 fatal landslides in a period between 1929 and 2019. However, there are no extensive studies on the regional economic effects of those landslides, and little have been done to bridge the gap. For this reason, this study aims at providing a framework of landslides hazard modeling and regional loss assessment. Due to the lack of detailed database in Turkey, we have chosen to use May 1998 Sarno debris flow in Italy as our case study.

May 5-6, 1998, Sarno debris flow was one of the unprecedented hazardous landslides that took place in the southern part of Italy with more than 160 fatalities and incurred huge financial loss [11]. It took place because of heavy and prolonged rainfall in the vicinity of Campania mountains. We have chosen this event as it typically represents a rainfall-triggered landslide in form of debris flow (i.e., flow type-landslide). Another reason for this choice is the availability and accessibility of the event data though it has been more than 25 years since it happened, researchers still use it till today ([12], [13], [14], [15]).

1.1. Literature Review Summary on Flood Hazard and Loss Modelling

Flood hazard can cause destruction of infrastructure, disruption of businesses and loss of life in the inundated areas[16]. Due to the increase in population growth, urbanization has expanded to normally unhabitable floodplains ([17]; [18]). The ever-changing world's topography and environment necessitate development of new techniques to accurately assess and mitigate flood hazard potential losses in any given area. One of the main steps towards flood risk management is flood hazard mapping. Through flood

mapping, flood prone areas are identified ([19]; [20]). Flood hazard mapping involves two main steps namely hydrological and hydraulic modeling ([21]). The next step to flood hazard mapping is to determine who would be affected or what would get damaged, and this is generally termed as exposure analysis ([22]). Flood damage is generally classified as direct and indirect damage[23]. While direct damages correspond to the direct effects of water on physical structures, indirect damage generally covers the effects of flood due to disruptions on people's activities [24]. These classifications can be subcategorized further into tangible and intangible damages ([25]). However, tangible damages are often transferred into monetary values and described in economic terms[26]. Several studies have attempted to quantify the relationship between structural damage of the exposed buildings to flood intensities such as flow velocity and water depth. Many studies postulate flood depth as the main indicator of building's incurred damage ([25],[26] ,[27],[28],[29],[30],[31]). However, there are other studies that have tried to quantify the building structural damage using other flood intensities such as velocity ([28],[29]), duration ([32],[33]etc. Numerous studies have been done to generate damage curves based on either empirical or synthetic data [34]. They include studies on England ([35]) on residential buildings in Czech Republic ([36]) on different buildings around the world [37], on 95000 buildings in New Orleans [38], etc. However, those damage curves based on only flood depth, though practical, have been criticized for failure to include all the flood parameters and the relevant uncertainties. These stage damage curves are mostly deterministic and limited in a way that they don't accurately predict the flood damages and their inherent uncertainties ([37], [38]). Ignoring those uncertainties can cause unreliable predictions on flood loss assessments and the flood consequences ([39].

Therefore, several studies ([32],[40], [41]) in literature have pointed out the need to bridge the gap since the lack of proper quantitative estimation of the related uncertainties can lead to wrong and unconservative calculations ([42], [43]). Moreover, there is a need for regional hazard loss models that estimate hazard losses of a community, not just individual buildings.

1.2. Literature Review Summary on Debris Flow Hazard and Loss Modelling

According to Varnes 1978 landslides classification, Debris flow: A debris flow is a form of rapid mass movement in which a combination of loose soil, rock, organic matter, and water mobilize as a semi-liquid mixture and flows downslope. Debris flows include <50% fines. Debris flows are commonly caused by intense surface-water flow, due to heavy precipitation or rapid snowmelt, that erodes and mobilizes loose soil or rock on steep slopes. Debris flows also commonly mobilize from other types of landslides that occur on steep slopes, which are nearly saturated, and consist of a large proportion of silt- and sand-sized material. Debris flow deposits are usually indicated by the presence of debris fans at the mouths of gullies. As it is the case for flooding, debris flow effects are escalated by the increase in population that has pushed people to settle in dangerous debris flow prone areas ([44], [45]). Recently, there is a growing number of studies in the literature on landslide hazard mapping ([46]. 2003; [47]) and so many others that seek to quantify their risk ([48], [49]; [50]). To determine the debris flow risk, a combination of the probability of the intensity and debris flow potential consequences in an area is needed.

The physical vulnerability of elements exposed to debris flow hazards is widely determined as the degree of damage of a given element and is generally quantified on a scale from 0 to 1, from no damage to complete damage respectively ([51]). For buildings, direct financial loss due to debris flow is often calculated by multiplying the monetary value to the vulnerability. This can be done based on the building market value ([52]; [53]; [54]) or based on the building reconstruction costs ([34]; [48]; [55]). There are so many studies on physical vulnerability of elements affected by debris flow and have suggested different formulation and damage curves that relate debris flow intensities, mostly inundation depth and velocities, to loss ([12], [35], [36]). Empirical methods are generally used to quantify physical vulnerability because analytical methods are generally complex and require detailed inputs which might not be practical [56]. Debris flow vulnerability assessment is often hampered by the presence of uncertainties as well as spatial variability because debris flows are inherently complex and can be difficult to accurately quantify them ([57], [58]). The main factors for the presence of those uncertainties can be the complex characteristics of the debris flow and limited information of their mechanisms, incomplete information of the building or property damages, lack of accurate observational debris flow's intensity data, and the presence of spatial and temporal variability of exposed elements. For these reasons, uncertainties associated with debris flow are hardly considered in debris flow hazard assessment [59].

1.3. Objectives

It can be easily inferred from the above discussion of literature review on both flooding and debris flow that there is a research need for comprehensive hazard loss assessment. Particularly in Turkey where few related studies have been attempted, it is imperative that

researchers redirect their effort towards flooding and debris flow hazard modeling and loss assessment as much effort has been deployed towards enhancing earthquake understanding and risk assessment. For this reason, this study attempts to pave a way to the many to follow research in the field. The objectives of this study can be summarised as follows:

- To model and assess the flood hazard risks on the town of Bozkurt as a case study.
- To model and assess the debris flow risk on the town of Sarno, Italy as a case study.
- To investigate the effects of considering uncertainties and spatial correlations on the overall regional flood and debris flow loss calculations
- To perform sensitivity analyses in order to understand effects of main parameters on loss assessment calculations.

1.4. Organization of the Thesis

This study has three chapters. In chapter 2, a framework for flood hazard modelling and risk assessment is discussed. The procedure for flood hazard loss assessments can be broken down into three main steps: hazard analysis, exposure analysis, and vulnerability analysis. In this study, flood hazard analysis is performed using Hydrologic Engineering Centre's Hydrologic Modeling System software (HECHMS) for hydrologic analysis and Hydrologic Engineering Centre's River Analysis System software (HECRAS) for hydraulic modeling, and the main goal of this is to produce flood hazard map. Flood exposure analysis is performed in a GIS program QGIS, and flood exposure map is the main output. Lastly vulnerability analysis is performed using three different flood-

damage relationships (Huizinga et al., 2017, Priska and Jonkman, 2010 and Maiwald et al.,2021). At this stage we also include spatial correlations and uncertainties, and their effects on total community financial loss is discussed. After applying and verifying using the August 2021 flood in Bozkurt, sensitivity analysis is performed, and flood discharge relationships to regional losses are proposed.

In Chapter 3, a procedure for debris flow hazard modelling and loss assessment is presented. As it is the case for flood, the procedure can also be summarized into three main steps: debris flow hazard analysis which is performed using Laharz software, debris flow exposure analysis in QGIS and vulnerability analysis performed using three different methods namely, Fachs et al. (2007), Kang and Kim (2016) and Akbas et al. (2018). In this chapter, effects of uncertainties and spatial correlations on overall regional debris flow loss are investigated. After that, we perform a sensitivity analysis to observe the effect a change in debris flow volume would have on the total cost.

Finally, the last chapter is about conclusion and necessary remarks on the contribution of this study, limitations, and suggestions on the future works.

CHAPTER II

FLOOD HAZARD MODELING AND LOSS ASSESSMENT

2.1. Introduction

Floods are one of the most destructive natural hazards that wreak havoc to society, structures, ecosystems, infrastructure, and to economy in general. According to WHO (World Health Organization), more than 2 billion people were affected by floods for a period of fewer than 20 years (1998-2017). According to [1], the global economic losses due to flooding are estimated to be more than one trillion dollars between 1980 and 2013.

Turkey has also been severely affected by floods over the past decades, and its effects are second to earthquakes only, but few studies have been conducted on flood hazard in Turkey. Within a period of 54 years (1960-2014), the Turkish disaster database has recorded over 1076 flood events that claimed over 795 people, incurring a total of $800 million financial losses [2]. Given the shear consequences of floods in Turkey, it is imperative that more studies are needed that are not limited only to hazard modeling but also seek to holistically assess and mitigate flood risks.

Additionally, flood risk modeling involves so many uncertainties and can significantly affect damage and cost estimations. The sources of these uncertainties are mainly due to generalizations, limited information and various assumptions made during the whole process of risk assessment [60]. There are so many studies in literature that have tried to quantify uncertainties such as [60], [61], [62], etc.

This article, therefore, seeks to quantify the economic damage caused by the flood considering the effects of uncertainties on the total loss estimations. We aim to establish

a framework for developing regional flood loss models in Turkey. As is shown by [63] ignoring uncertainties leads to nonconservative results. There is, therefore, a need to include uncertainties associated with flood loss estimation. This paper also incorporates the effects of spatial correlations due to similar flood demands and similar building conditions to aggregate individual building losses into a total loss estimate.

Using the flood event that took place on 11th of August 2021 in Bozkurt (in Black Sea region of Turkey) as our case study, we provide an easy-to-follow framework of flood hazard modelling and loss assessment. Moreover, we also try to estimate the effects of uncertainties and spatial correlations on the total replacement costs associated with flood damage on buildings.

2.2. Case Study

Bozkurt is a small town (Figure 1), located in Kastamonu Province within the Black Sea basin of Turkey. The Ezine Stream, which originates approximately 2 km away from the Black Sea, serves as the main drainage system for Bozkurt Water basin covering a watershed area of around 275 km^2. According to data from the Denizli Chamber of Commerce, Bozkurt had a population of approximately 12,000 people in 2020. The region experiences higher average annual precipitation of 1214 mm mainly because of its mountainous topography, proximity to the Black Sea coast, and overall high humidity compared to other regions surrounding Bozkurt that receive about 450 mm of precipitation annually [64]. Additionally, the flood risk in Bozkurt is intensified by the fact that so many buildings are built within the floodplains along the banks of the Ezine Stream.

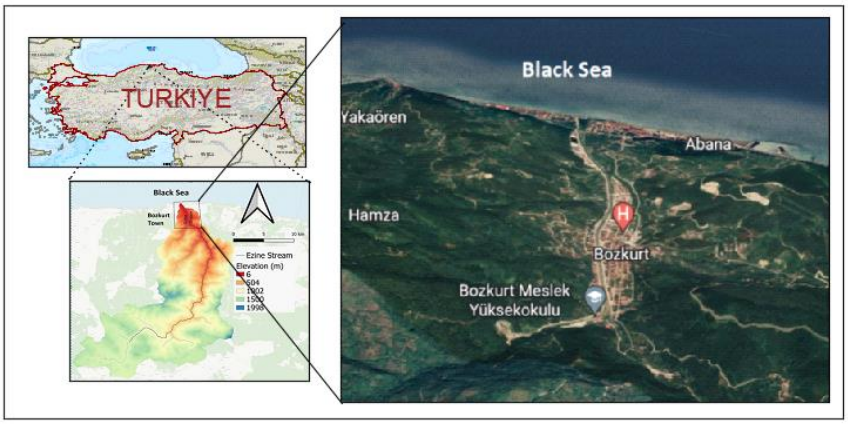

Figure 1. Location of the town of Bozkurt in Kastamonu, Turkey

On the 11th of August 2021, the place experienced an unprecedented flood following a two-day torrential rainfall. The flood affected so many places in the Black Sea Basin (Northern Parts of Turkey), its death toll was as high as 71 lives in the Bozkurt Town alone. The flood also has caused so much property damage including destruction of infrastructures like bridges, buildings and disruption of other economic activities as discussed by [3]. We have chosen Bozkurt as our case study because it is one of the most recent flooding events in Turkey. Figure 2 and Figure 3 are some of the images taken during and after the August 2021 flood in the town of Bozkurt.

Figure 2. Aerial photograph during August 2021 flood in Bozkurt, Turkey ([65])

Figure 3. Photos showing the water depth of the Bozkurt Flood on some buildings [66].

2.3. *Methods*

The framework of flood hazard modelling and loss assessment comprises three main steps: namely flood hazard analysis, exposure analysis and vulnerability analysis as shown in Figure 4.

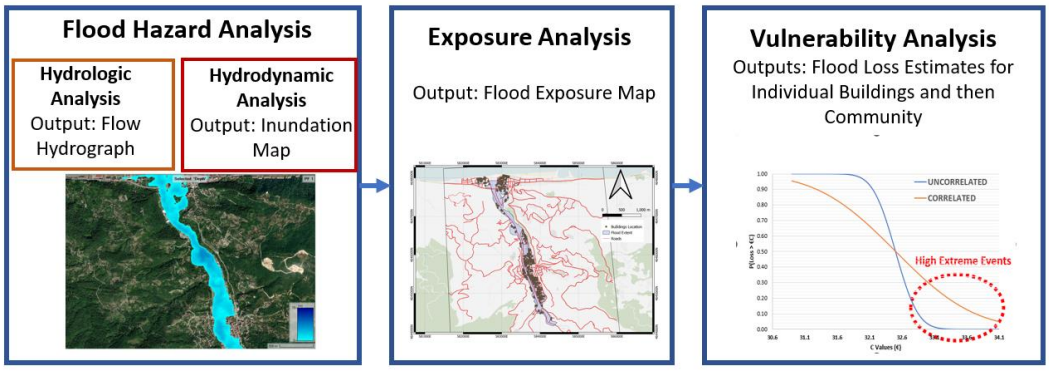

Figure 4: Flood loss modelling procedure

2.3.1. Flood Hazard Analysis

2.3.1.1 Hydrologic Analysis

Proper hydrologic analysis is crucial for the development of hydrodynamic analysis and other ensuing processes. One of the widely used programs for hydrologic analysis is HEC-HMS (Hydrologic Engineering Centre-Hydrologic Modeling System) developed by

the US Army Corps of Engineers (Figure 5). HEC-HMS is a hydrologic modeling program that can be used for flood forecasting, water resources management, or stormwater management within a given drainage area [67]. It allows the users to define `basin's physical characteristics such as soil types, channel geometry and land use, meteorological data like precipitation and evaporation to estimate runoff, river flows, and other hydrologic parameters. HECHMS can be used to simulate both event based and continuous hydrologic models.

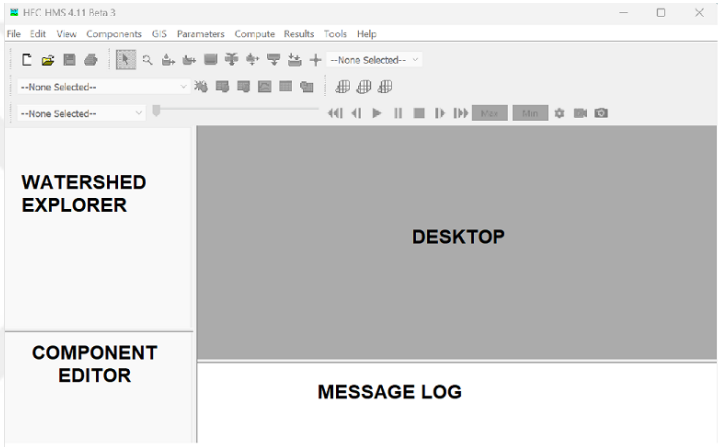

Figure 5. Diagram showing components of HEC-HMS interface.

According to HEC-HMS USACE User's Manual (2018), modeling in HEC-HMS consists of four main files for simulation:

1. Project file: a file containing basic information about the project like project name, version of the model, time zone and names of the data.
2. Basin file: file containing physical properties of the basin, like stream network, connectivity, methods, and parameters for hydrological process simulations.
3. Meteorologic file: this file saves information about weather input.

4. Control specification file: contain information about the simulation time (when simulation starts and stops, and time interval)

We begin with creating a new project file and setting up the unit system, SI units in our case. We then add terrain data by uploading our DEM into the program. In our case a 30-m resolution downloaded from STRM is used. After uploading DEM, basin model is created, and GIS coordinate system of the project is selected (UTM 36N zone is selected for Bozkurt). By processing drainage, the program will automatically create flow accumulation and flow direction. We then delineate streams which will work on the flow accumulation grid by specifying the stream area thresholds which were taken as 10 km^2 for in this study. To delineate the basin and its subbasins, an outlet (break point) is specified, and then subbasins and reaches are delineated. The identified subbasins and reaches are displayed in the watershed explorer section and their characteristics such as river length, subbasins areas, and slope and basins slopes are stored (Figure 6). We can pre-process the subbasins by merging some of them or doing other necessary modifications.

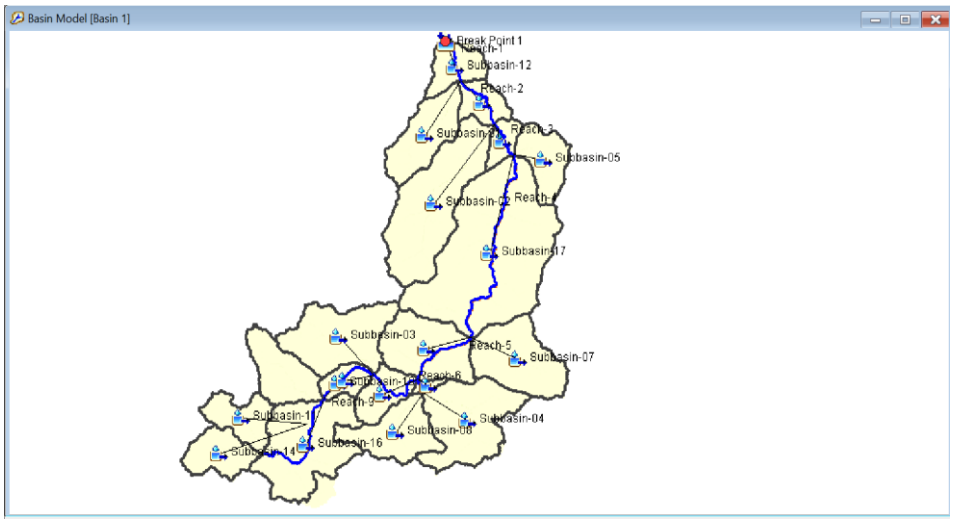

Figure 6. HEC-HMS delineated model reaches and subbasins of Ezine river watershed.

The procedure for rainfall-runoff hydrologic modeling in HEC-HMS involves four main methods:

- **Loss Rate Methods:** There are so many loss methods but, in this study, Soil Conservation Service Curve Number (SCS CN) loss method is used. SCS CN method estimates excess rainfall as a function of parameters like soil cover, cumulative precipitation and land use using the equation below [67]:

$$Pe = \frac{(P - Ia)^2}{(P - Ia) + S} \tag{2.1}$$

Where Pe is the accumulated excess precipitation at time t, P is the accumulated rainfall depth at time t, and I_a is the initial loss, and S is the potential maximum retention. Unless the initial abstraction is exceeded by the accumulated rainfall, the precipitation excess is zero. An empirical relationship has been developed between I_a and S and it was found that I_a =0.2*S. Using the watershed's curve number as an intermediate parameter, the program calculates the maximum retention (S) using the following equation [67]:

$$S = \frac{25400 - 254\ CN}{CN} \tag{2.2}$$

Where, S is the maximum retention in SI units and CN is the watershed's curve number, a value that ranges from 100 to around 30, representing water bodies and permeable soils respectively. CN number depends on several parameters like land use and soil type. Following the study of [3], CN is taken to be 65 for the case study. Another parameter needed for SCS Curve Number loss method is percentage of impervious area and it is assumed to be 5% for Bozkurt watershed [3].

- **Transform Methods**: these are methods that allow the modellers to convert the rainfall hyetographs (after subtracting losses) into streamflow hydrographs. HEC-HMS offers nine choices that include unit hydrograph methods, a linear quasi-distributed method, a kinematic wave implementation, and a two-dimensional (2D) diffusion wave method. In this study, Soil Conservation Service (SCS)unit hydrograph transform method is used. There is one main parameter used for SCS Unit Hydrograph transform method: namely, lag time.

$$Tc = \frac{l^{0.8}(S+1)^{0.7}}{1.140\,Y^{0.5}} \quad (2.3)$$

$$Lag = 0.6\,Tc \quad (2.4)$$

where, Lag is the lag time in hours, Tc time of concentration in hours, l is flow length in ft, Y is average watershed slope, and S is the maximum potential retention in inches.

Lag time is calculated for each subbasins (Table 1), and the values are entered in HEC-HMS.

Table 1: Calculations subbasins' Lag time

Subbasin	L(km)	Y, slope	CN	S	Y, %	Tc(hr)	Lag(hr)
Subbasin-01	10.24	0.41	65	5.38	41.06	2.06	1.23
Subbasin-02	15.20	0.40	65	5.38	39.88	2.86	1.72
Subbasin-03	10.70	0.32	65	5.38	31.60	2.43	1.46
Subbasin-04	11.49	0.27	65	5.38	27.40	2.76	1.66

Subbasin-05	6.25	0.44	65	5.38	44.02	1.34	0.80
Subbasin-06	4.45	0.50	65	5.38	49.90	0.96	0.57
Subbasin-07	8.99	0.43	65	5.38	43.23	1.81	1.08
Subbasin-08	9.79	0.30	65	5.38	29.76	2.33	1.40
Subbasin-09	5.58	0.46	65	5.38	45.57	1.20	0.72
Subbasin-10	9.66	0.22	65	5.38	21.97	2.68	1.61
Subbasin-11	7.39	0.20	65	5.38	19.66	2.29	1.37
Subbasin-12	5.95	0.34	65	5.38	33.92	1.47	0.88
Subbasin-13	6.45	0.36	65	5.38	36.12	1.51	0.91
Subbasin-14	7.19	0.21	65	5.38	20.97	2.17	1.30
Subbasin-15	9.39	0.33	65	5.38	33.40	2.13	1.28
Subbasin-16	11.31	0.19	65	5.38	19.20	3.26	1.95
Subbasin-17	19.89	0.45	65	5.38	45.31	3.33	2.00
Subbasin-18	3.14	0.33	65	5.38	33.46	0.88	0.53
Subbasin-19	5.52	0.38	65	5.38	38.20	1.30	0.78

- **Baseflow Methods**: In HEC-HMS, subbasin element consists of the interaction of surface runoff, infiltration, and subsurface runoff. The subsurface runoff calculations are done by baseflow methods. HEC-HMS offers six baseflow methods to choose from. If baseflow methods is not selected, the subbasin will not compute baseflow and the outflow will only include direct runoff from the transform method. In this study, we have chosen the “None Method”, meaning that we there is no selected baseflow method.

- **Routing Methods**: This involves selecting reach routing method. This is a method used to predict the changes in shape of a hydrograph as water moves through a river channel or a reservoir. There are quite several routing methods in HEC-HMS, but we have selected Kinematic Wave Routing Method. We have chosen this method because of the absence of observed data and the physical characteristics of the studied area. This method uses unsteady flow equations but ignores pressure and inertial forces. It is often suited for urban areas with modified natural stream channels. This method requires the user to enter parameters like shape of the channel, manning coefficients, length, index flow (expected maximum flow), and slope of the channel, etc.

After basin model, the user enters data for meteorological model. The main purpose of this step is to specify the meteorologic boundary conditions of each subbasin [67]. The user can specify each subbasin's model or can use the model to more than one subbasin. In this model the user can choose either precipitation, evapotranspiration, snowmelt, or longwave radiation methods. In this study, we have used precipitation data from the meteorological station around Bozkurt namely, Abana, Kuz and Mamatlar Rain gauge stations as shown in the Figure 7. The average of the hourly precipitation data recorded on 11-12 August 2021 was calculated and then are entered into the program. Using the Thiessen polygon method, the gages precipitation weights are calculated and entered in HEC-HMS.

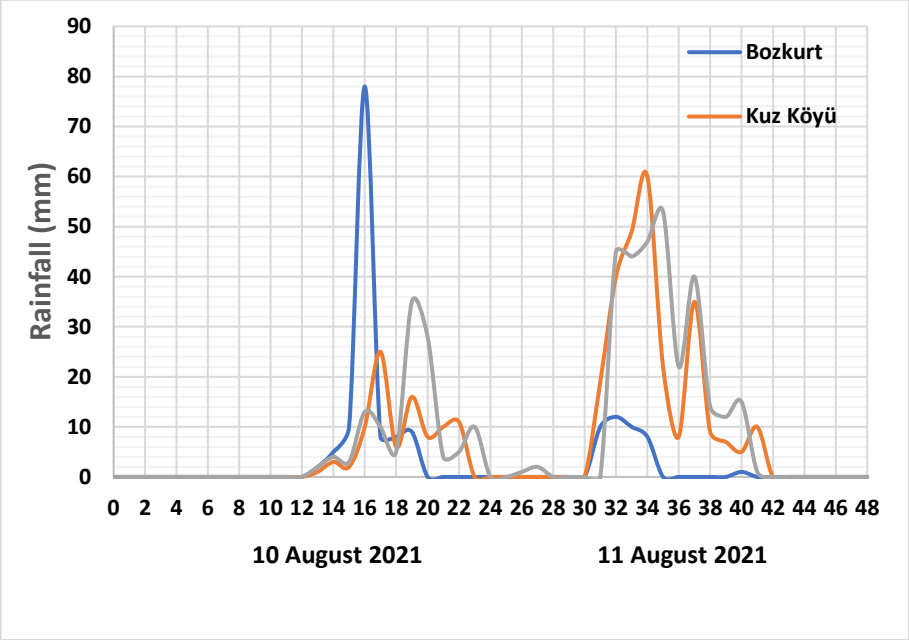

Figure 7. Rainfall hyetographs for the three rain gauge stations in Bozkurt vicinity. [68].

Next, a control specifications file is created. The main purpose of this file is to specify the start time, end time and the time interval used in the simulation. The hydrologic analysis in HEC-HMS gives a hydrograph with peak discharge of 1102 m^3/s. The result of this hydrologic analysis is validated by comparing the peak discharge and the shape of the hydrograph with the results in the study done by [3] in which the peak discharge was found to be 1026 m^3/s (Figure **8**).

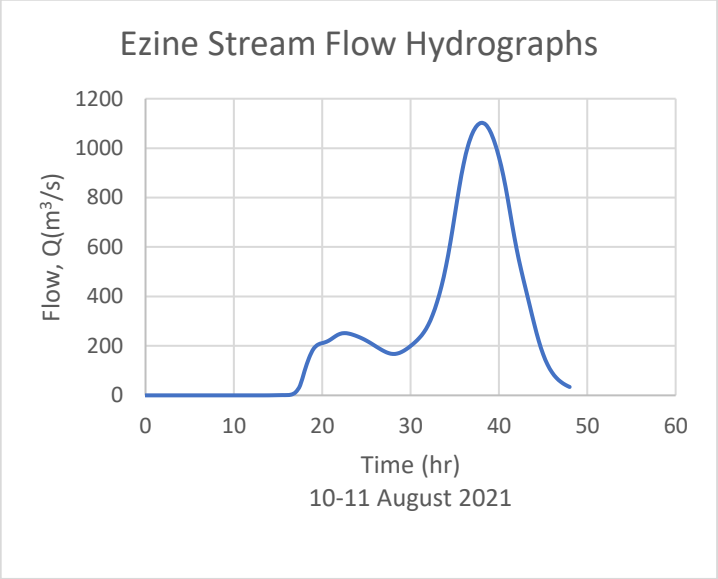

Figure 8. Simulated flow hydrograph of Ezine stream

2.3.1.2 Hydrodynamic Analysis

The hydrograph obtained from hydrologic analysis serves as a boundary condition for hydraulic analysis. We have also appropriated HEC-RAS (Hydrologic Engineering Centre's River Analysis System), to perform hydrodynamic analysis. HEC-RAS is another software developed by the US Army Corps of Engineers, mainly for river analysis. It has the capabilities of performing 1D steady as well as 1D and 2D unsteady flow analysis [69]. Creating Hydraulic model in HEC-RAS can be summarized in five main steps: (1) starting a new project, (2) entering geometric data, (3) entering flow data and boundary conditions, (4) performing hydraulic simulations, and (5) viewing the results. Running Hydraulic simulations in HEC-RAS needs four main files (Figure 9):

1. **Project file**: a file containing basic information about the project including names, units of the project and other relevant or default information.
2. **Geometry file:** a file containing basic information about the river or reach schematics, cross-section profiles, hydraulic structures (e.g., bridges and culverts), manning coefficients, and modelling approach information.

3. **Flow (steady/unsteady) file**: file containing information of the flow and boundary conditions.
4. **Plan file**: file containing information like the description and short identifier for the plan, list of files associated with the plan, and information of the simulation options.

Depending on the type of the analysis, we might also have sediment data file, Quasi-Unsteady flow data files, water quality data files, and hydraulic design data files (**Figure 9**).

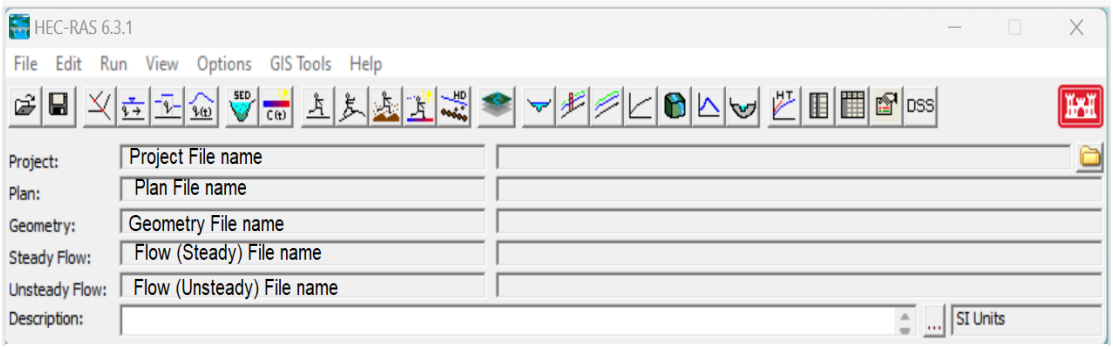

Figure 9. The HEC-RAS main window interface

HEC-RAS solves energy equation (Equation(2.5)) to calculate water surface profiles from one cross section to the next with a standard step method (Figure 10).

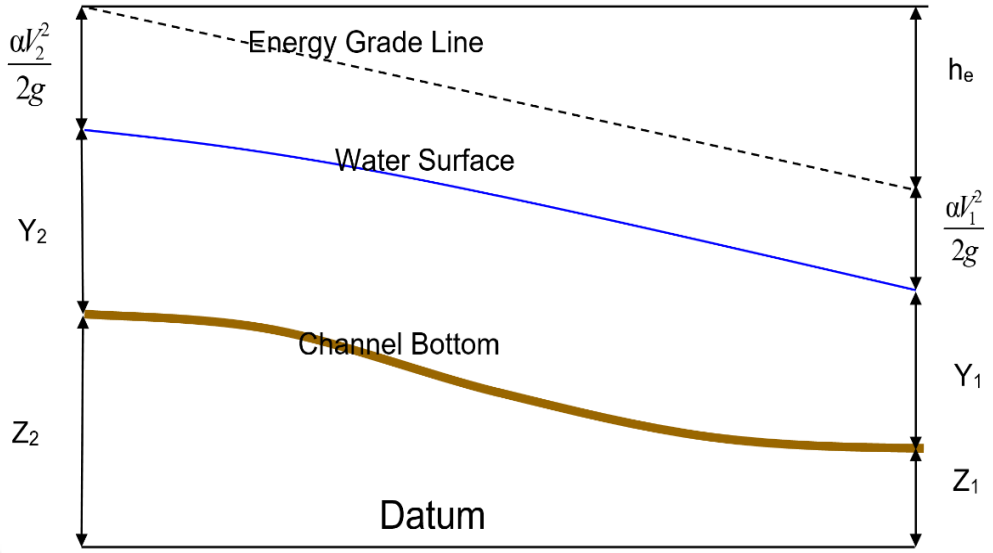

Figure 10. Representation of terms in energy equations.

$$Z2 + Y2 + \alpha 2\frac{V2}{2g} = Z1 + Y1 + \alpha 1\frac{V2}{2g} + he \tag{2.5}$$

Where Z1/ Z2 are elevation of the main channel inverts, Y1/Y2 and V1/V2 are water depths and average velocities at the cross sections respectively, α1/α2 are velocity weighing coefficients, g is gravitational acceleration, and he is energy head loss.

The energy head losses are calculated by taking account of friction and contraction/expansion losses as shown in Equation (2.6):

$$he = L\bar{S_f} + C\left(\frac{\alpha_2 V_2^2}{2g} - \frac{\alpha_1 V_1^2}{2g}\right) \tag{2.6}$$

Where L is discharge weighed reach length, $\bar{S_f}$ is friction slope between the two sections, and C is the contraction/expansion loss coefficient.

HEC-RAS also uses Manning's equation (see Equation (2.7) below) to calculate the flow Q on each section of the river reach:

$$Q = \frac{1.486\ A*R^{\frac{2}{3}}*S^{\frac{1}{2}}}{n} \tag{2.7}$$

where Q is the flow rate, A is the flow area, R is the hydraulic radius, n is manning roughness coefficient, and S represents friction slope.

To begin hydraulic modeling in HEC-RAS, we import Digital Elevation Model (DEM), in GeoTiff format (with geo-reference coordinate system). Newer versions of HEC-RAS have GIS capabilities and DEM can be directly imported into its RAS Mapper. Geometry file is created and modified in RAS Mapper. Here, river channels, cross-sections, riverbanks, and floodplains are defined (**Figure 11**). The geometric data are drawn based on the google imagery that can be imported into HEC-RAS GIS Mapper.

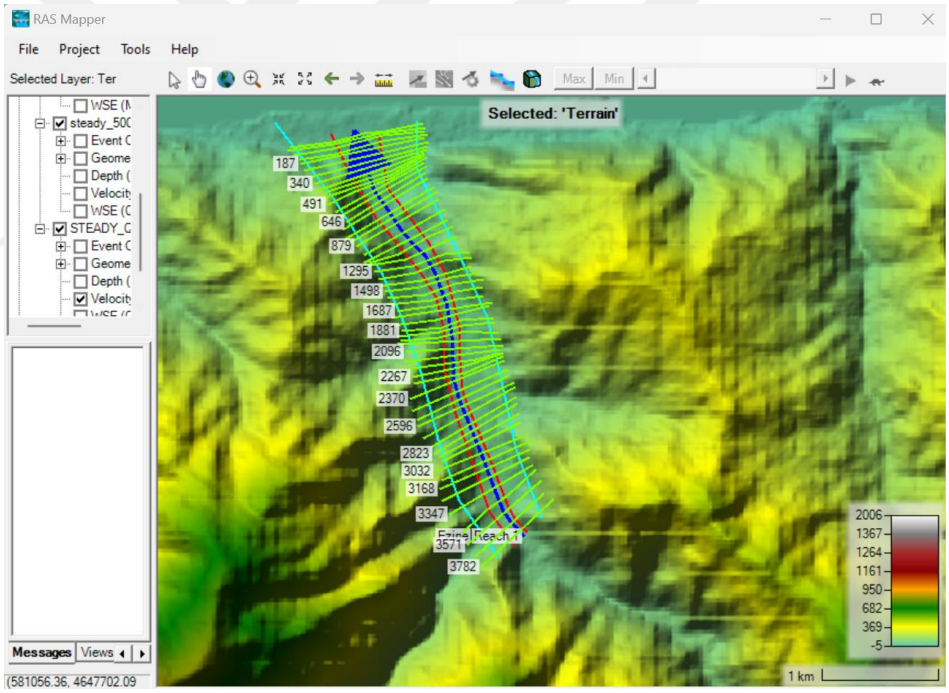

Figure 11. Diagram for Ezine River geometry in Bozkurt town in RAS Mapper.

Next, we specify the manning coefficients for each cross-section. The manning coefficients used in this study are taken from the values provided on USACE websites [67] and it suggests that the manning value of 0.035 for riverbed, 0.1 for forests, 0.08 for urban areas and 0.04 for bare soil The hydraulic simulation is performed using 1D

unsteady flow analysis and we have used the hydrograph obtained from the hydrologic analysis as the upstream boundary condition and normal depth where we entered channel slope as the downstream boundary condition. The results were validated by comparing the results to the models in other works like and using photographs taken from the events as shown in Figure 12. It was reported by [70] in part a of the figure that the water depth reached 1 meter high while it reached 5 meters in part b. From our hydraulic analysis we have found that the water depth in part a was ranging between 0.83 m to 1.17m and 4.2m to 4.44m in part b. Moreover, the inundation map obtained in this study was compared to other studies in the same region ([71],[72]) and it can be clearly concluded that our results are in agreement with those other studies. HEC-Ras can produce flood inundation map for both velocity and water depth.

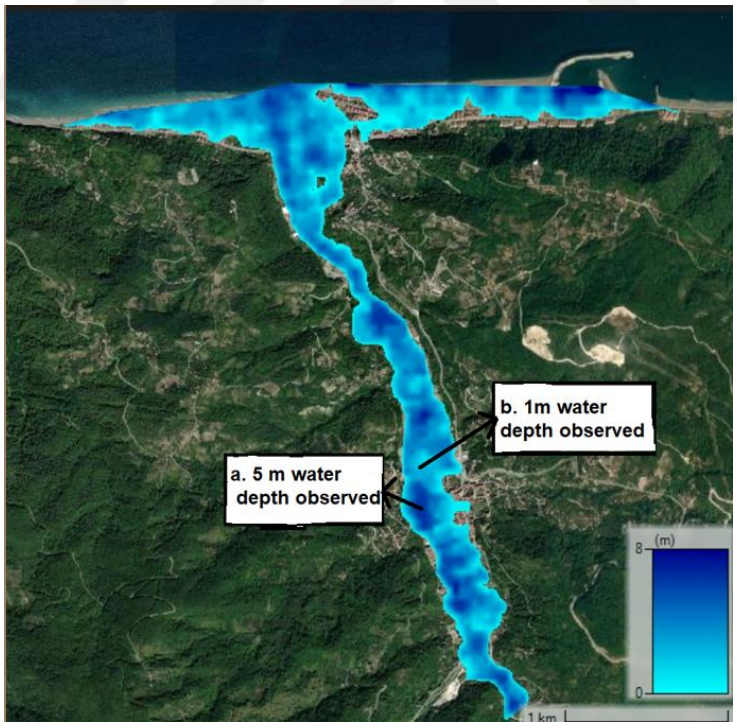

Figure 12. Bozkurt town's flood hazard map showing inundation depth.

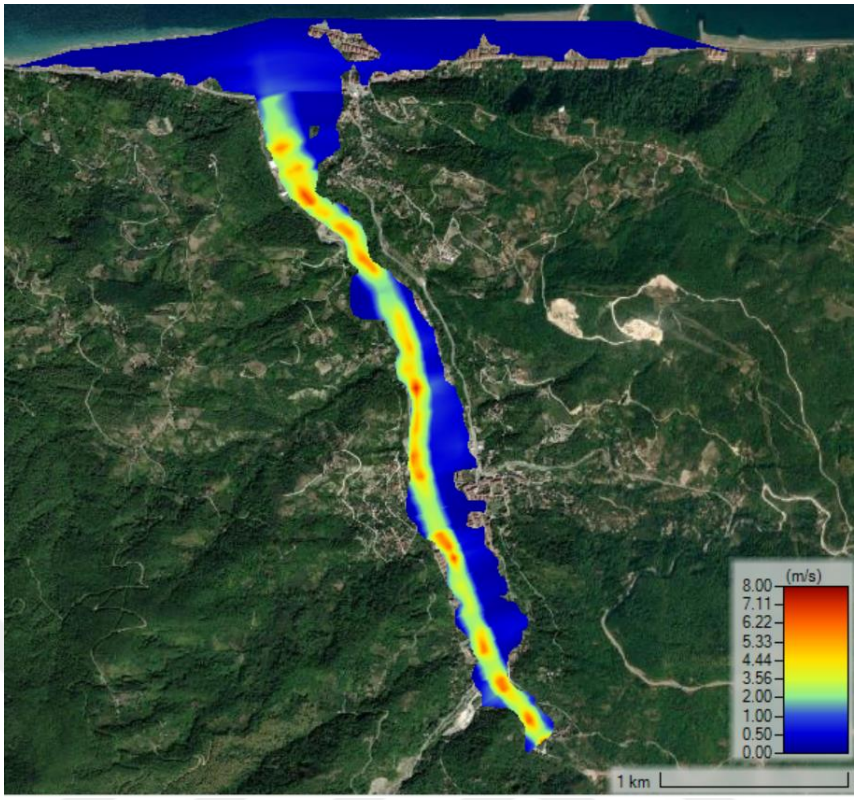

Figure 13: Bozkurt town's flood hazard map showing flow velocity.

2.3.2. Exposure Analysis

Exposure flood hazard analysis is defined as a process of quantifying the number of buildings exposed to flood hazards and it is an important step towards flood risk assessment [73]. After the flood hazard analysis in which inundation map is the desired data, we proceed with exposure analysis. This step is done using Quantum GIS(QGIS), a publicly available GIS software and can be readily downloaded from Google [74].

Using QGIS software, flood hazard extent raster layer is uploaded. This part involves determination of building features such as building location, building area, building type (e. g. residential, commercial), and building material used are identified. So, a shapefile containing building footprints is prepared. We have prepared this building information shapefiles using information from Google Earth [75], Google imagery and

Google Open Street Maps [76]. Hence the building information provided lack depth as to what construction material used, number of stories of the buildings and age of the buildings. It is only limited to the building's footprint area and only to building categories are considered, residential and commercial buildings.

The flood intensities affecting each building (velocity, and water depth) are found by superimposing the building feature and flood hazard map separately as shown in Figure 14 below. It can automatically be performed in QGIS using a plugin called "Sample Raster Values."

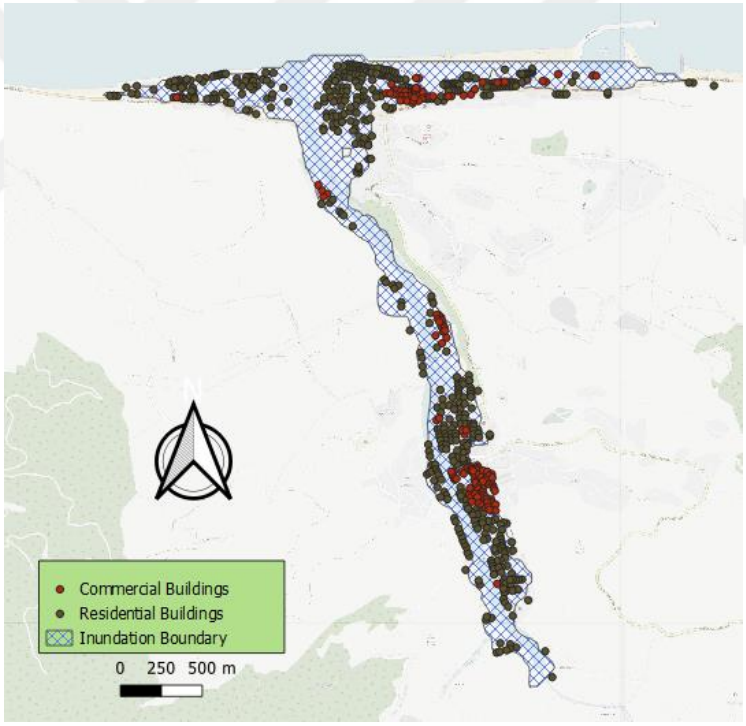

Figure 14: The August 2021 flood extent map for the town of Bozkurt

2.3.3. Vulnerability Analysis Results

At this stage, the damage due to flood hazard is transformed into economic loss or repair costs. There are so many studies on the economic value for a microscale flood damage assessment [77], but they mainly fall into two categories. They are either empirical where

actual flood damage data is used or synthetic approaches that uses hypothetical analysis based on extrapolation. It is beyond the scope of this study to discuss in depth the difference and the reliability of each approach, but it can be mentioned that empirical approach is the most used approach in the construction of damage curves, thanks to its high implementation rate [77]. There are so many damage curve functions in the literature, and they utilize different flood intensities, mainly flood depth and flow velocity. In this study, we use three different flood damage functions, and they are separately discussed below.

2.3.3.1 Huizinga et al. (2017)

Huizinga damage curves are one of the popular and most used damage curves worldwide. It is an extensive study that provides water depth-damage curves for each continent and for so many countries across the globe. Figure 15 shows water depth-damage relationship on residential, commercial, and industrial buildings for European countries.

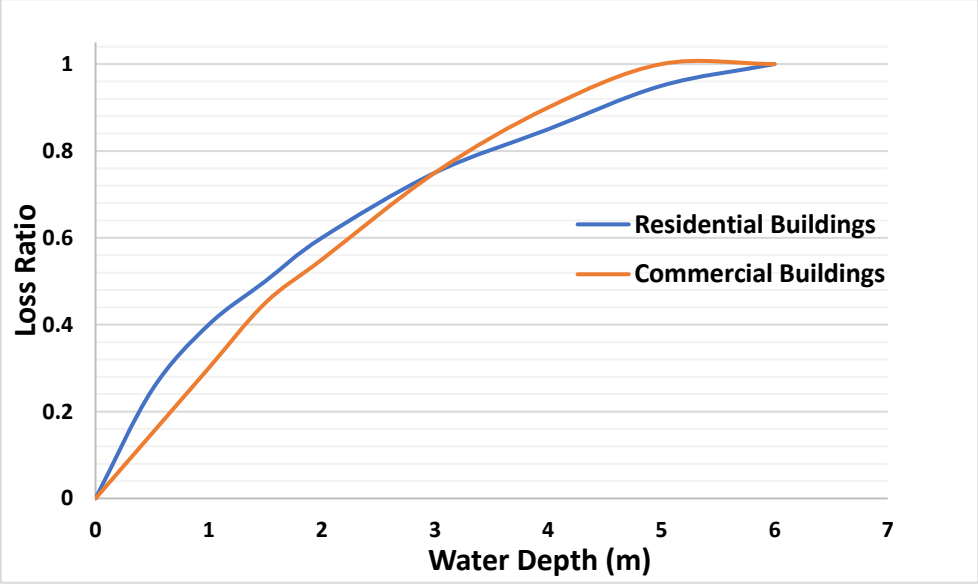

Figure 15: The flood depth-damage curves assumed in the study (Huizinga et al., 2017)

2.3.3.2 Pistrika and Jonkman (2010)

Using the empirical dataset of 2005 flooding of New Orleans of about 95000 buildings, [30] propose a relationship between flood damage and its incurred financial damage to residential buildings. Pistrika and Jonkman (2010) predicts damage percentage using formula (2.8:

$$D = 0.457 + 0.063dv^{0.654} \quad (2.8)$$

where D, d and v represent the food damage factor (%), food depth (m) and velocity (m/s), respectively.

2.3.3.3 Maiwald et al. (2022)

After a series of studies, a comprehensive and detailed flood-structural damage relationships are developed based on the damage data from the 2002 Germany flood combined with the 2011 Tohoku earthquake in Japan[31]. The formulation proposed is multivariate and we have chosen the equations which are based on inundation height and/or velocity (equations (2.9) & (2.10)). In this study the formula constants are modified to calculate damage states. Table 2 shows the calculated damage states and the assumed loss ratios.

$$\mathrm{D} = 4 * \tanh(0.238.\,\mathrm{d} - 0.914) + 3 \quad (2.9)$$

where d represents inundation level or specific energy height; and

$$D = 4 * \tanh(0.062.\,d + 0.042.\,dv - 0.647) \quad (2.10)$$

where d is the inundation level and v represents flow velocity [31].

Table 2: A table of damage states and the study's assumed loss ratios

Damage State (DS)	Loss Ratio
0	0
1	0.5
2	0.8
3	0.92
4	1

Having recorded individual building damage percentage, and buildings' surface area, replacement cost is calculated using the three methods mentioned above. The replacement unit values of residential and commercial, are €454/m^2 and €656/$m^{2,}$ respectively as suggested by [29]. Huizinga damage curves estimate the total cost of €32.5 million which is based on only water depth, Pistrika and Jonkman formulation estimates of the total repair cost is €37.3 million, while Maiwald estimates a total cost of €34.5 million and €37.8 million based on the equation (2.9) and equation (2.10) respectively (Figure 16), €33.96 million estimated by Priska and Jonkman (2010), €21.6 and €32.08 million using Maiwald et al. (2022) equation (2.9) and equation (2.10) respectively. Moreover, following the premises found in the study by [3] that the August 2021 flood in Bozkurt was way higher than a 500-year flood of the region, we have sought to find out that this argument is equally reflected on the financial losses as well. Following the same procedure, the 500-year flood repair cost is calculated, and the results are compared as reflected on the graph (Figure 16). From the graph, the replacement costs of the August 2021 Bozkurt flood are way higher in comparison to the estimated costs in case of a 500-year flood, thus reinforcing the argument by [3]. It can also be seen that the formulations that consider both water depth and velocity into account give high estimates compared to the relationships that only consider inundation depth.

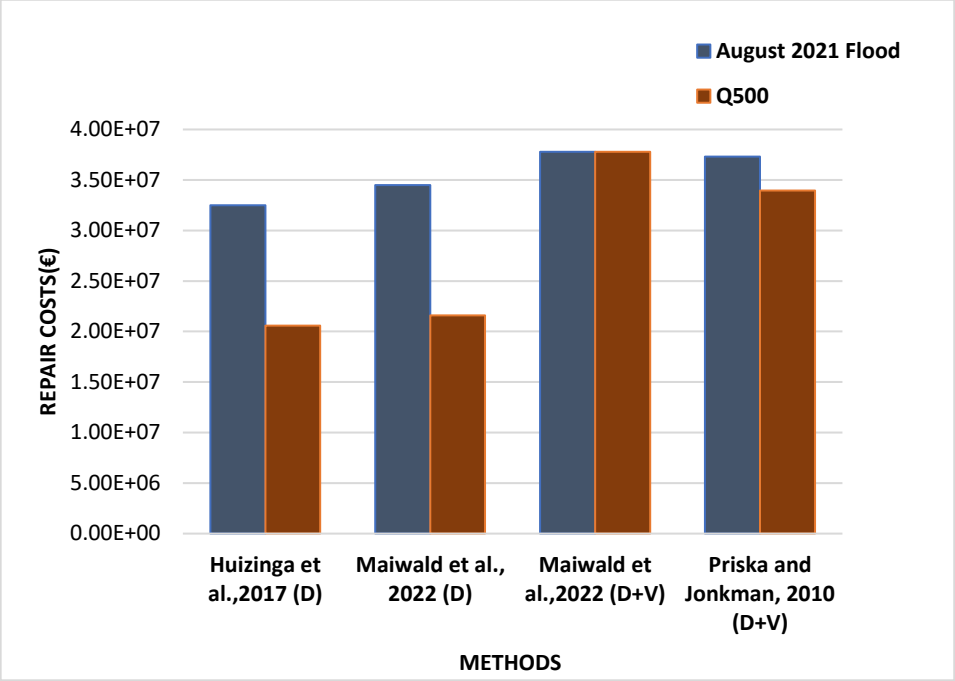

Figure 16. Comparison of flood damage costs of the 11 August 2021 Bozkurt, Türkiye flood to Q500 flood damages using different methods.

To demonstrate the effects of uncertainties and spatial correlations on the community flood loss estimates, we have used the formulations proposed by [63] study. The spatial correlation is calculated based on the distance between each individual pair of buildings in the flood extents (Equation (2.11 & (2.12). We have assumed a COV (coefficient of Variance) of 0.3 for each individual building, correlation distance of 1km, and the distribution is assumed to be a normal distribution.

$$E[L_T] = \sum_{i=1}^{N} E[L_i] \tag{2.11}$$

$$Var[L_T] = \sum_{i=1}^{N} Var[L_\iota] + \sum_{i=1}^{N} \cdot \sum_{j=1}^{N} \cdot \rho_{Li,Lj} * SD[Li] * SD[Lj] \tag{2.12}$$

Where E[Li] is the expected loss values, SD[Li] and Var [Li] are the standard deviations and variances respectively. $\rho_{Li,\ Lj}$ is the correlation coefficient and is calculated as shown by Equation (2.13) below:

$$\rho_{Li,Lj} = exp^{-r_{i,j}/r_o} \quad (2.13)$$

Where r_o is the correlation distance and is assumed to be 1km in this study.

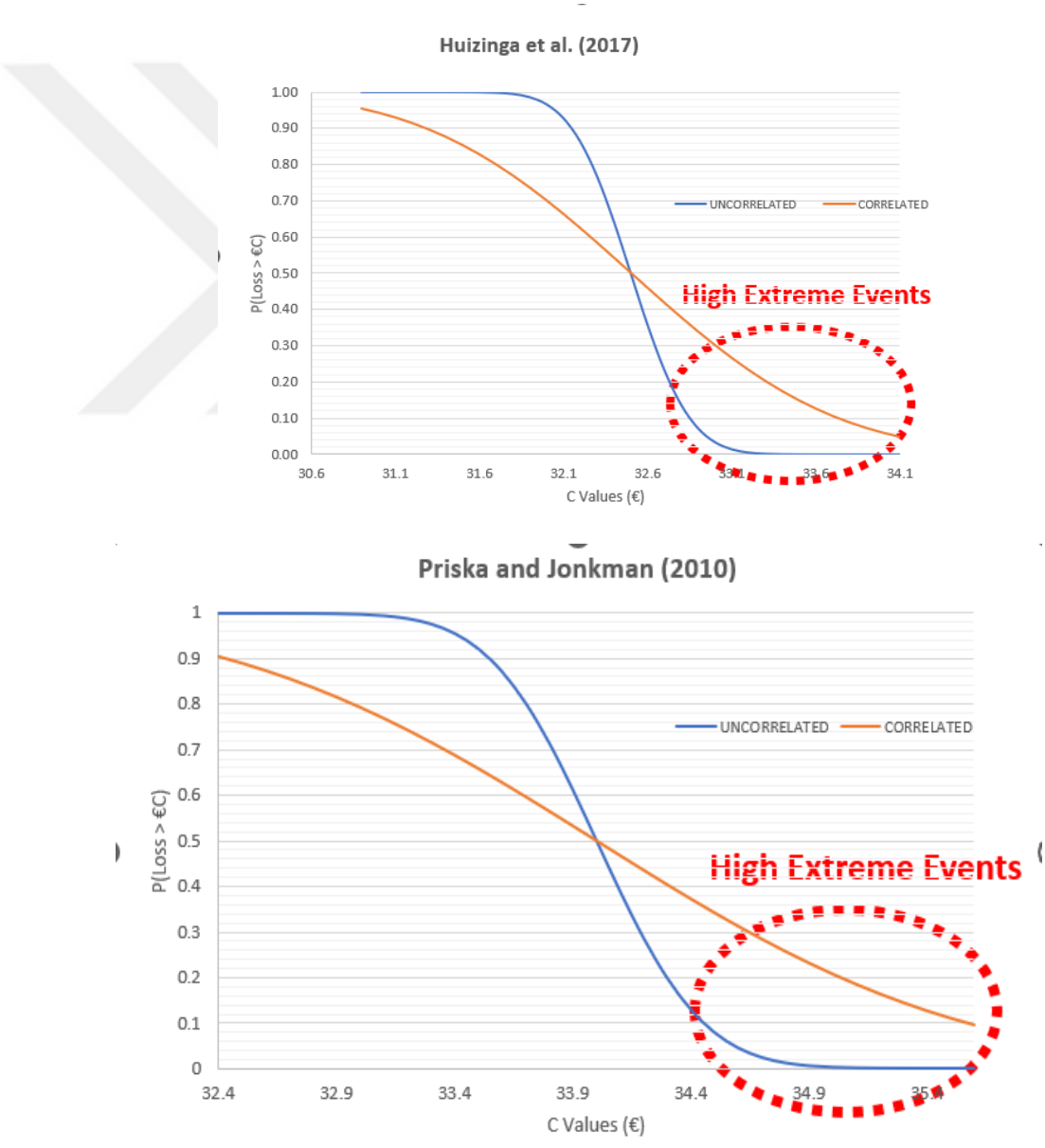

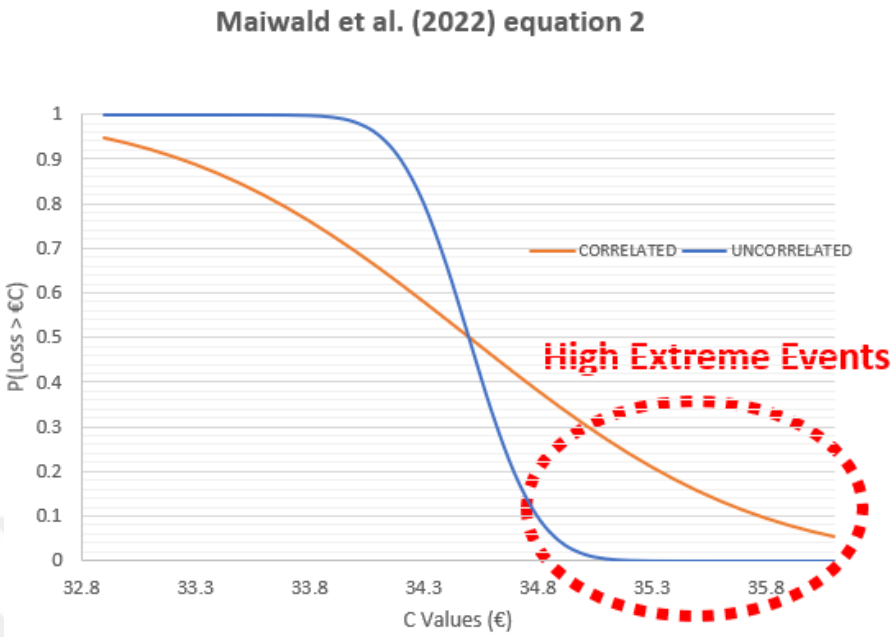

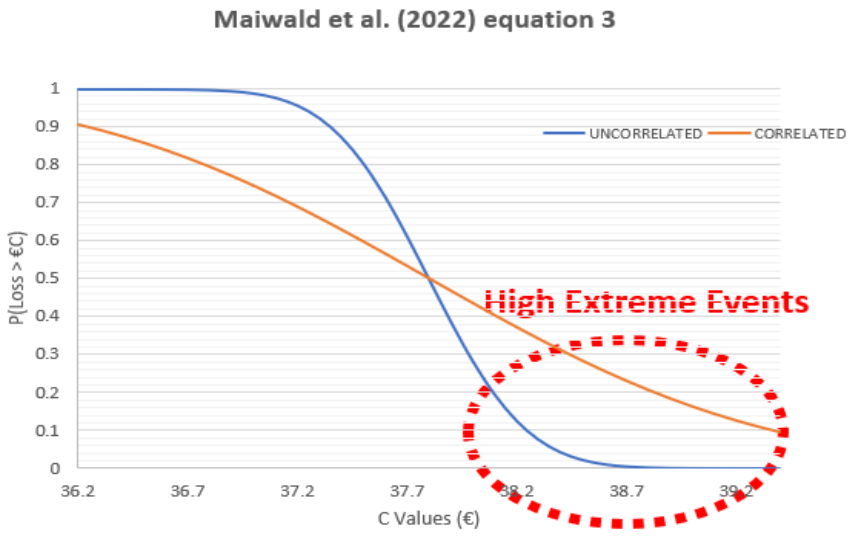

Figure 17. Probability of exceedance for the aggregated flood losses using a. Huizinga et al. (2017), b. Priska and Jonkman (2010), c. Maiwald et al. 2022 (Equation (2.9)) and d. Maiwald et al. 2022(Equation (2.10)).

The Figure 17 represents the probability that the total costs will exceed the calculated costs using the three methods discussed above. As presented in the figure,

ignoring uncertainties and spatial correlations can lead to non-conservative loss estimates for high-extreme events.

2.4. Sensitivity Analysis

After establishing a framework for flood hazard modeling and loss assessment, a sensitivity analysis is performed to establish a relationship between flow discharge and aggregated financial loss of the town of Bozkurt. This part aims at providing a quick but efficient way of estimating regional financial loss in the aftermath of a flood catastrophe which in turn will help in quick fund allocation, in risk identification, regional master planning, and in development of national resilience policies.

First, we begin by establishing a reasonable range for flood discharge values. [78] has done a comprehensive study of hydrologic and hydraulic modeling of the town of Bozkurt using both the data before and after the August 2021 flood event. As outlined in previous sections, we have followed the same procedure to prepare inundation maps for each of the listed flow discharges and have added few other values that fall in the range between 91 m^3/s to 2046 m^3/s, Q2 and Q1000 of the Ezine Stream watershed for both 2years and 1000years return periods respectively (Table 3). Moreover, we have also used the four different flood loss estimations formulations, namely Huizinga damage curves [29], Priska and Jonkman formula [30], Maiwald equation (2.9) and equation (2.10) respectively [31]. The resulting financial loss estimates using the four discharge-loss relationships are recorded in Table 3 below. To proceed, the results are graphed and mathematical representations of the water discharge-loss relating equations are sought.

Table 3. A table of discharge values used for the sensitivity analysis and their corresponding calculated damage costs using the four different methods.

Estimated Damage cost (Million €)					
Discharge, Q (m3/s) ([78])		**Huizinga et al. (2017)**	**Priska and Jonkman (2010), equation** (2.8)	**Maiwald et al. (2022), equation** (2.9)	**Maiwald et al. (2022), equation** (2.10)
Q_{2a}	**91**	6.41	31.20	7.5	26.16
Q_{2b}	**105**	6.98	31.30	8.7	26.39
Q_{5b}	**175**	9.70	31.75	11	27.48
Q_{10a}	**225**	11.30	32.06	12.5	28.2
Q_{25a}	**292**	13.95	32.53	14.9	29.19
Q_{50b}	**345**	15.65	32.78	16.4	29.86
Q_{10a}	**358**	16.00	32.90	16.8	30.02
Q_{100b}	**397**	17.15	33.13	18	30.52
Q_{500b}	**527**	20.60	33.95	21.6	32.08
Q_{25b}	**570**	21.56	34.19	22.7	32.6
Q_{50a}	**765**	26.00	35.35	27.4	34.7
Q_{100a}	**990**	30.62	36.71	32.4	36.93
2021 Flood	**1100**	32.50	37.30	34.5	37.8
Q_{500a}	**1575**	40.55	40.08	43.2	42.03
	1600	41.00	40.20	43.6	42.24
	1680	42.20	40.60	44.9	42.89
	1750	43.20	41.00	45.9	43.43
	1850	44.50	41.56	47.5	44.2
	1920	45.33	41.90	48.5	44.74
Q_{1000a}	**2046**	47.00	42.60	50.1	45.56

* The subindices ‘a’ and ‘b’ correspond to the Q values for different return periods (in years) obtained by [78] ‘after’ and ‘before’ the 2021 Bozkurt flooding, respectively.

It is concluded that the relationship can be represented by a power function using Huizinga flood loss method (**Figure 18**). Hence Equation (2.14) below is proposed for community financial flood loss estimation on the town of Bozkurt using Huizinga et al.

(2017). The premise is strengthened by the fact that the corresponding R-squared (coefficient of determination) of the equation is 0.9993, implying a nearly perfect correlation.

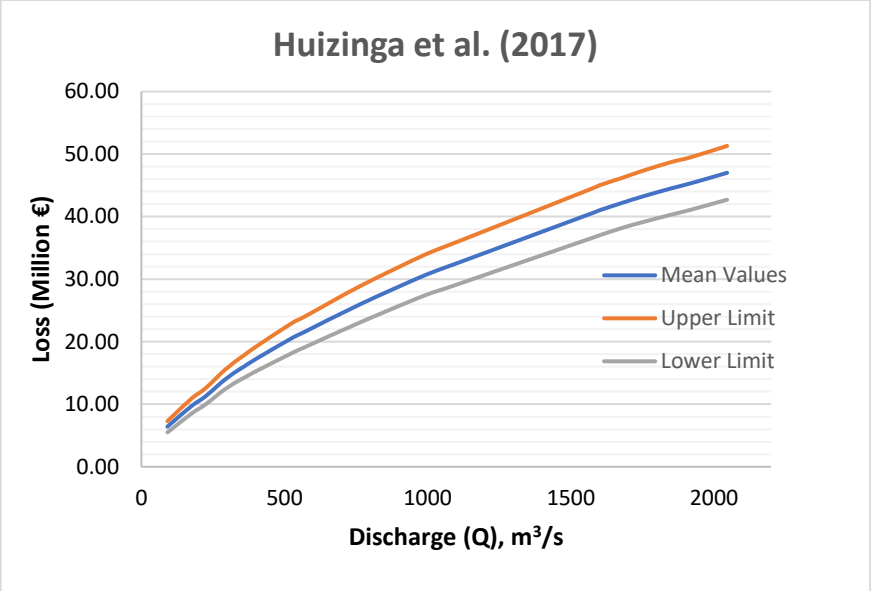

Figure 18. Graphical representation of the relationship between flood discharge values and estimated financial loss for the town of Bozkurt using Huizinga damage curves (note: upper and lower limits correspond to the bounds of a 90/10 two-sided confidence interval respectively)

$$L = 0.357 * Q^{0.643} \tag{2.14}$$

where L represents aggregated financial loss, and Q represents maximum flood discharge of Ezine Stream in the town of Bozkurt.

It is also realized that there is a linear relationship between flow discharge and loss values using Priska and Jonkman method ([30]) with a coefficient of determination of 0.9996 (Figure 19). Thus, Equation (2.15)) is proposed.

$$L = 0.0058 * Q + 30.8 \tag{2.15}$$

Where L represents aggregated financial loss, and Q represents maximum flood flow rate of Ezine Stream in the town of Bozkurt.

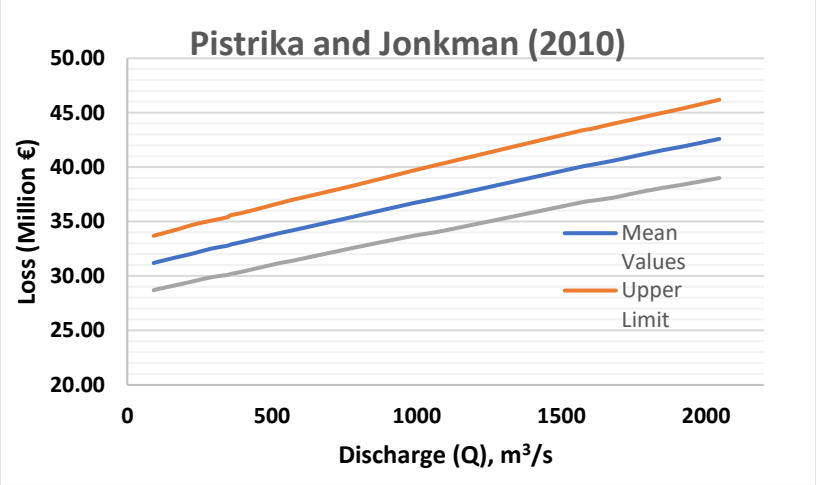

Figure 19. Graphical representation of the relationship between flood flow rate values and estimated financial loss for the town of Bozkurt using Priska and Jonkman method (note: upper and lower limits correspond to the bounds of a 90/10 two-sided confidence interval respectively)

Using Maiwald Equation(2.9) and Equation (2.10) methods [31], it is found out that there losses can be estimated using a power function relationship with a coefficient of determination of 0.9996 and a linear relationship with a coefficient of determination of 0.9928 respectively (Figure 20 & Figure 21). To estimate the flood loss of the region of Bozkurt using Maiwald et al. (2022) methods Equation(2.16)and Equation (2.17) are suggested.

$$L = 0.464 * Q^{0.614} \tag{2.16}$$

$$L = 0.0058 * Q + 30.8 \tag{2.17}$$

where L represents aggregated financial loss, and Q represents maximum flood flow rate of Ezine Stream in the town of Bozkurt.

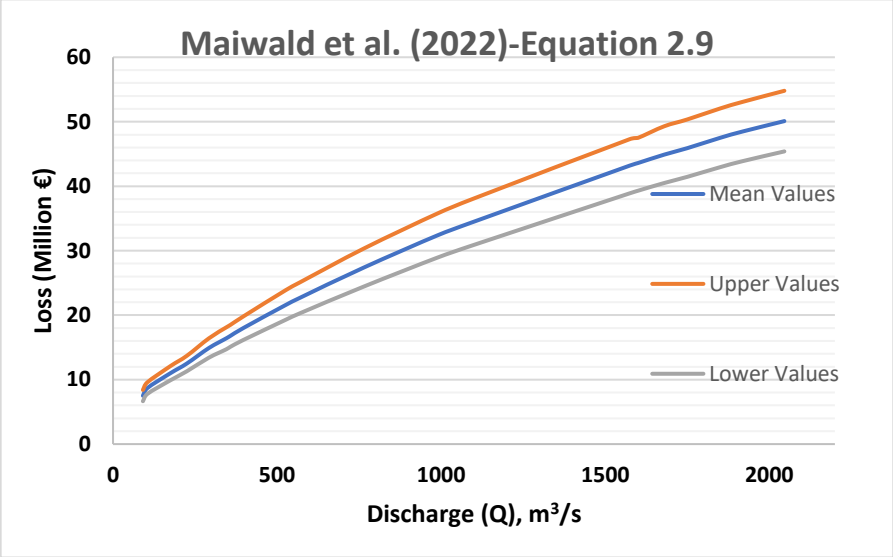

Figure 20. Graphical representation of the relationship between flood flow rate values and estimated financial loss for the town of Bozkurt using Maiwald Equation (2.9) (note: upper and lower limits correspond to the bounds of a 90/10 two-sided confidence interval respectively)

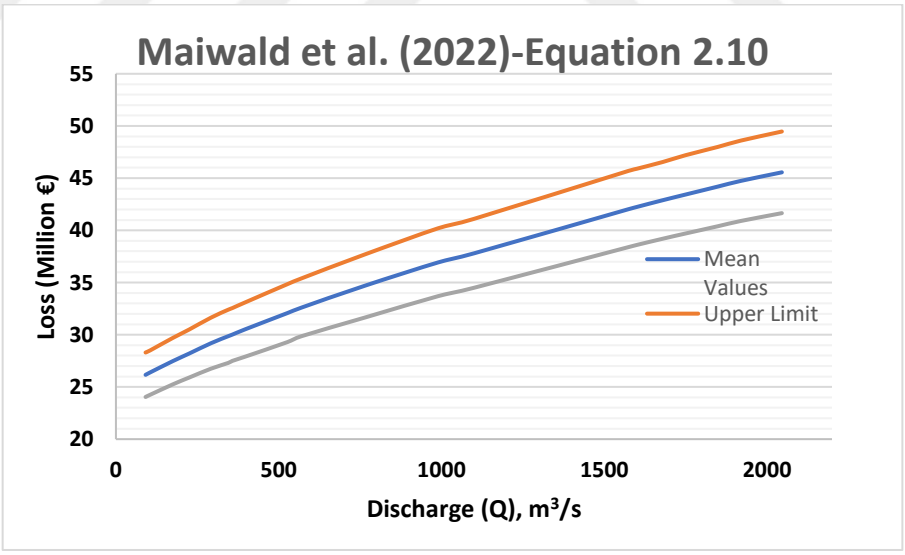

Figure 21. Graphical representation of the relationship between flood flow rate values and estimated financial loss for the town of Bozkurt using Maiwald Equation (2.10) (note: upper and lower limits correspond to the bounds of a 90/10 two-sided confidence interval respectively)

CHAPTER III

DEBRIS FLOW HAZARD MODELING AND LOSS ASSESSMENT

3.1. *Introduction*

Landslides are one of the most disastrous natural hazards. They can cause significant damage to infrastructure, the economy, and society at large. According to the Global Landslide Catalog [4], there were over 11,000 fatal landslides worldwide between 2004 and 2016 resulting in the deaths of over 56,000 people. Globally, there have been over 1.6 million deaths and around $260-310 billion of economic loss every year since 1990 [5]. The estimated economic losses from those landslides were approximately $10 billion per year worldwide between 2004 and 2016. To put this into perspective, the 2008 earthquake triggered landslides in Wenchuan alone causing more than 80,000 deaths [79]. In addition to the immediate impacts of landslides, they can also have long-term consequences such as increased erosion and sedimentation, which can affect water quality and damage infrastructure over time [80].

Given the fact that landslides, especially those triggered by rainfall [4], have been causing global damage, it is of vital importance that researchers should turn their attention to landslides risk management. Landslide risk assessment is a crucial step in landslide risk management, which involves the identification of hazards, estimation of the likelihood of occurrence, and assessment of the potential consequences. There is a growing body of literature on landslide risk assessment, which reflects the increasing awareness of the importance of managing landslide risk. The literature can be broadly

categorized into three main steps: (1) hazard identification and mapping ([81]; [82], (2) vulnerability analysis ([83]; [84], (3) risk analysis [85].

To begin with, it is important to first clarify what we mean by some of the specific terms that we use in this work. There are so many definitions of landslides, debris flows, mudflows and so many related terms which are interchangeably used by many people in literature as discussed by [86]. Perhaps the most accepted definition and classification of landslides was proposed by [87] which was later modified by [88] works. In their work, landslides are defined as the movement of the saturated or oversaturated mass of either earth, rock, or debris down an incline [87]. Landslides classification is based on source material type, water content, rate of movement (velocity), and the type of movement (slide, flow, spread, etc.) [87]. According to Varnes' classification [87], the first term describes material type whereas the second term describes the type of movement. Thus, debris flow and debris slide are two different categories. According to material type, landslides are divided into rocks, debris, mud, earth, and soil whereas fall, topple, flow, spread, and slide are the distinct divisions of landslides according to their kinematic types of movements. With this, we may have earth spread and earth slide, debris flow, debris slide, rock topple, and rock fall.

Since it is beyond the purpose of this work to examine the connotations of each subdivision, we stick to the flow types of landslides. According to Varnes' 1978 study on landslides [87]there are five distinct classes of flows namely: (i) debris flow: Varnes' (1978) definition of debris flow is "a very rapid to extremely rapid flow of saturated debris in a channel, composed of a mixture of water and rock fragments derived from any source and ranging in size from clay to boulders. (ii) Mudflows which is defined as a flowage of

at least 50 percent fine-grained earth material with a liquid limit exceeding 25 and having a high degree of plasticity. (iii) earth flows are defined as a downslope movement of soil or rock debris exhibiting both shearing and flowing; it is usually characterized by a broad, spoon-shaped, or tongue-shaped shear head carp, backward rotation of the displaced material, and undulating surface flow.

Other internationally recognized classifications of landslides such as [89] and [90] agree with much of Varnes's classifications [87], especially on the flow types of landslides. For this reason, we have adapted the definitions and classifications mentioned above. However, our study only deals with debris flow.

Numerical simulations of debris flow require rigorous and complex analysis and remain unpractical in engineering applications ([91], [92]). For this reason, many studies use semi-quantitative methods of debris flow assessment ([93]). Debris flow models generally treat the mixture of water and solids as a single fluid component with specific rheological properties, and typically use one of three types of constitutive equations to determine flow resistance: Bingham laminar flow, Newtonian turbulent flow, or dilatant grain shearing in the inertial regime. [94] as well as [95] conducted a comparative analysis of basic modeling approaches. [93] has proposed a five-steps semi-quantitative procedure based on numerous debris flow events and analyses that had occurred in Switzerland. Those steps are (i) Calculation of debris flow volume (V), (ii) Estimation of peak discharge (Q_p), (iii) Calculation of velocity (v), (iv) Flow cross-section area (A), and (v) calculation of total travel distance (L) and runout distance on a fan (L_f). There are so many empirical formulations used to estimate each of the above quantities and are discussed in the ensuing sections.

3.2. Case Study

On May 5-6, 1998, following a series of heavy and prolonged rainfall, Campania experienced unprecedented landslides hazard that claimed around 160 deaths causing approximately $100 million property loss [11]. Campania is a small town in the southern Italy province of Salerno, with a population of around 17,000 (Figure 22). It is one of the regions in which the Apennines Mountain ranges pass. The landslides occurred due to rainfall that triggered volcaniclastic top layer of about 0.5-2 m to slide down the valley resulting in a very rapid debris flow. There have been so many slope stability problems leading to landslides tracing back as far as 1632. But the May 1998 Sarno event was unlike the others because it was a series of landslides with more than 1,500,000 m^3 mobilized flow mass volume [11] through several channels (Figure 23). There are several factors that can trigger debris flow including earthquake, rainfall, weathering etc. [96]. Examples of rainfall induced debris flow events are found all over the world: in Italy [97], in Mexico [98], in Colombia [99], etc. It was shown by hydrological analysis that the May 1998 Sarno Debris flow in the Southern parts of Italy was triggered by rainfalls [100]. The Sarno rainfall-induced landslides have been classified as debris flow by so many studies in the literature including ([11], [97]). [96] has done an extensive study of the analysis of the May 1998 Sarno landslides sources and the geotechnical modelling of the triggering mechanism. [100] has discussed possible explanation of the causes of the May 1998 Sarno debris flow:

1. Because of the pumice's voidity and lack of packing for more fine ash particles (the material is less dense).
2. The coarseness of the pumice particles and the unloaded arrangement of the ash that cause the grain mass to act like a collection of angular fragments.

3. Soil suction which is partially influenced by the presence of permeable limestone bedrock and characterized by a karstic surface. This karstic nature resulted into the drainage of the overlying mantle deposits.
4. The presence of vegetation in the places where pyroclastic deposits fell.

In this work, the May 1998 Sarno debris flow hazard was modelled using LAHARZ software [33] and estimated the incurred economic loss due to building damages. There have been studies that have modelled the Sarno debris flow hazard but, to the knowledge of the author, there is no study that has estimated the building damages loss in monetary terms.

Figure 22. Regions of May 1998 Sarno Landslides [101].

Figure 23. Photographs of a. the 1998 Sarno debris flow channels [12], b. scoured channel because of rapidly moving debris flows [102].

3.3. Methods

The framework used for debris flow hazard and loss assessment resembles that one of flood hazard (see Section 2.3), and it can be summarized into three main steps: Debris flow hazard analysis, debris flow exposure analysis and vulnerability analysis (see Figure 24. Debris flow hazard modelling and loss assessment procedure

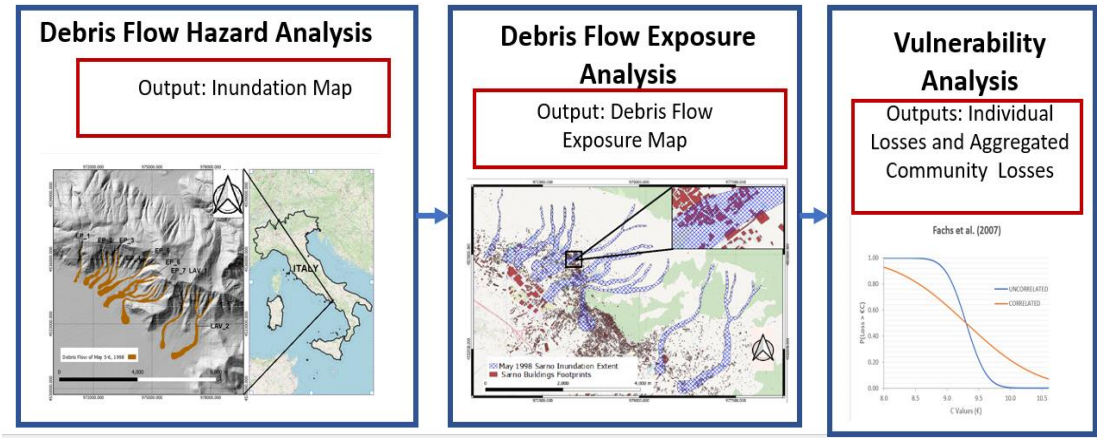

Figure 24. Debris flow hazard modelling and loss assessment procedure

To begin with, for a better understanding of the procedure, let's shade light on some important concepts on the methods used for debris flow analysis as described in the proceeding section flow hazard analysis.

- **Debris Flow Volume and Peak Discharge Estimation Methods**

First, debris flow analysis starts with the estimation of debris volume as it is the basis for debris flow peak discharge, the total runout distance, and the total travel distance estimations [93]. There are quite a lot of techniques in the literature used to estimate debris flow volume [103]. The most used techniques include GIS-based techniques [104], photogrammetric techniques [105], and empirical methods ([106], [93]). The empirical methods were proposed based on the morphometric characteristics of the drainage area.

Studies conducted earlier have indicated that there exists an empirical correlation between the volume of debris flow (V) and the maximum discharge of the debris flow (Qp) (as demonstrated by [107], [108], and [93]. Some commonly used formulas include:

i) Rickenmann (1999) formula:

$$Qp = K\ V_d^{0.833} \quad (3.1)$$

where Qp is the peak discharge, V_d is the volume of the debris flow, and K is an empirical coefficient which equals 0.1 [93].

In the case study, Rickenmann equation has been used.

ii) Hungr's formula:

$$Qp = K*V_d^{0.5}, \quad (3.2)$$

where Qp is the peak discharge, V_d is the volume of the debris flow, and K is an empirical coefficient. Hungr's formula is based on the field measurements of debris flow in British Columbia, Canada [107].

iii) Mizuyama et al. (1992)'s formula:

$$Qp = K*V_d^{0.78} \quad (3.3)$$

where Qp is the peak discharge, K is empirical coefficient which equals to 0.135 for granular debris flows and 0.0188 for muddy debris flows, b is taken. Mizuyama's formula is based on field measurements of debris flows in Japan [108].

- **Flow Velocity Calculations**

Debris flow is known for its ability to travel long distances, cause significant damage, move at high speeds, and leave large amounts of debris in alluvial fans. Researchers in the field of Geo-hazards have shown a great interest in understanding the dynamic features of debris flow. Analyzing the factors that affect the run-out and physical characteristics of debris slurry is an essential aspect of studying this phenomenon. Parameters such as peak discharge, volume, impact force, velocity, and material

properties play a crucial role in understanding debris flow. Velocity is particularly important for mitigating the hazards caused by debris flow, as it affects the distance travelled, impact force, and the time taken for debris to reach the alluvial fan. The estimation of velocity is, therefore, a critical factor in preventing and mitigating the damages caused by debris flow, and any mitigation structure needs to consider the velocity of the flowing mass.

In hydrodynamics, there are several methods for estimating longitudinal flow velocity. However, due to the highly complex and unpredictable nature of debris flow, conventional velocity estimation procedures are not always effective. Only a limited number of methods have been used to determine the velocity of debris flow. These methods can be broadly classified into two categories: (1) velocity approximation using analytical methods and (2) Field investigations, which involve real-time monitoring or back-calculation based on superelevation [109]. There are also many analytical methods formulations in the literature, and they include exact solution methodologies for a fully 2D channel flow ([110], [111]), mean formula calculation methods [112], and the recent two-phase fluid model method as discussed by [113]. However, the above analytical formulation requires rigorous studies and lacks the practicality that empirical methods offer. The most used and well-known empirical method is the super-elevation method which is often used for the practical analysis of debris flow [109].

The super-elevation method involves measuring the amount of lateral displacement of a debris flow in a curved channel and using this measurement to estimate the velocity of the flow. This method assumes that the debris flow follows a circular path and that the centrifugal force acting on the flow is balanced by the gravitational force.

The velocity of the flow can then be calculated using Chow 1959 velocity equation which was later improved by some studies that suggested the addition of a correlation coefficient ([107], [114],[115]) described in **Figure 25** below :

$$V = (K * g * R * \Delta e/w)^{0.5} \quad (3.4)$$

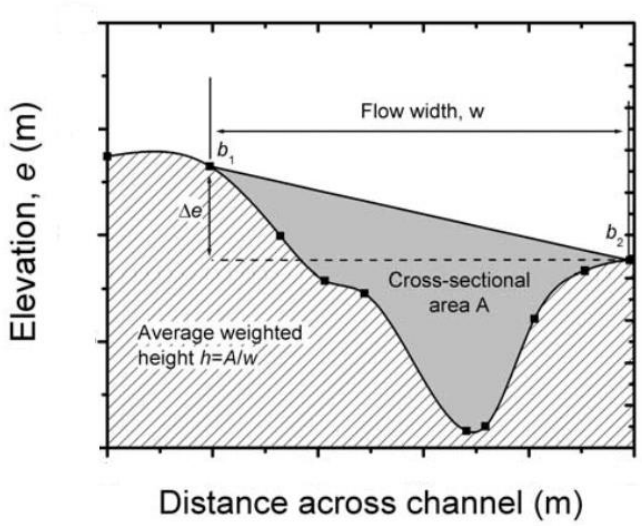

Figure 25. Cross profile illustration of superelevation method ([115])

Where V is the velocity, g is the acceleration due to gravity, R is the radius of the curved channel, w is the channel width, K is the correlation coefficient and Δe is the difference in elevation between the inner and outer banks of the channel.

It should be noted that this method has some limitations and uncertainties, as it assumes a uniform flow and neglects the effects of flow turbulence and roughness. Therefore, it is recommended to use this method in combination with other methods to obtain more accurate velocity estimates. It should also be noted that the key characteristic of debris flow is the presence of a channelized or confined flow as discussed by [89], thus the above formulation of debris flow velocity can also be termed as confined flow velocity.

Perhaps, one of the challenges involved in the use of this method is the estimation of the radius of curvature which is a subjective measurement in natural channels. There is a lack of detailed discussions on how to estimate bend radius in technical writings, except for a study by [116], which highlighted the challenges involved in determining the radius. [117] and [118] discuss the derivation of unconfined alluvial fan flow velocity using the kinetic potential energy equation. This assumes a total transformation of kinetic energy into potential energy. The unconfined flow velocity equation is given below:

$$V = (2 * g * \Delta h)^{0.5} \quad (3.5)$$

Where g is the gravitational acceleration, and Δh is the distance between the ground surface and the energy line.

Additionally, as discussed by [93], maximum velocity can be calculated using flow peak discharge. Even though equation (3.6) is based on clear water analysis, it has been shown that it can also be used to estimate debris flow maximum velocity [119].

$$Vmax = 2.1\ Qp^{0.33} S^{0.33} \quad (3.6)$$

Where S is the local slope and Qp is the peak discharge.

- **Runout Distance Calculations**

The total travel distance and runout distance (Figure 26) might be of much interest especially to roughly delineate debris flow endangered zones [93]. A parameter that illustrates the ability of debris flow to move down a slope is called mobility of the flow (L/ΔH). This parameter is only based on the ratio of the height difference to the distance between the source and the deposit area [120].

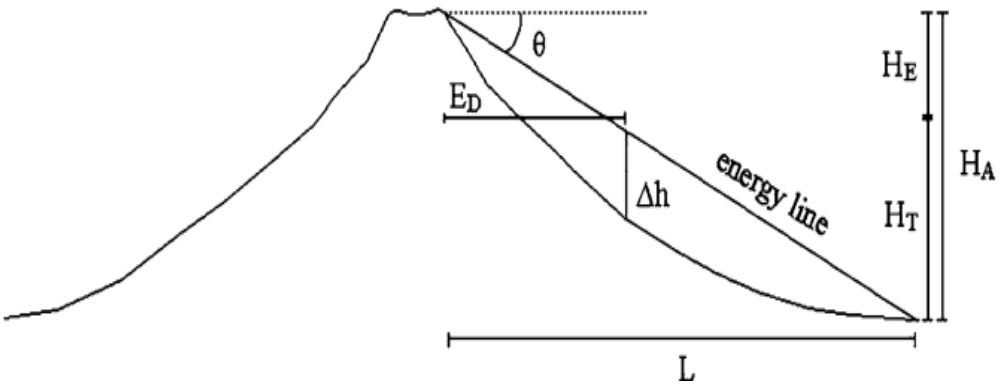

Figure 26. Diagram illustration of the energy line concept. ΔH is the drop in the height over runout distance (L). ED is the Euclidean distance from the source point, HT (the energy line elevation) = HA – HE, Δh= HT – DEM-elevation [120].

Different studies ([91]; [93];[121]) have indicated that there is quite a relationship between the mobility ratio and the volume of the debris, and that one can be used to estimate the other. [91] mentions that the boundary conditions and geometry of the runout path are the main factors affecting the mobility ratio, thus runout distance.

- **Debris Flow Modelling by LAHARZ**

Debris flow is a non-Newtonian fluid, and its mechanics are complex due to the interaction between particles and the fluid. There are quite several debris flow modeling software like FLO-2D (a widely known debris flows modelling software that considers the factors like soil properties, local slope, water content to predict debris flow mechanics) and RAMMS which stands for Rapid Mass Movement Simulation is also used to simulate debris flow, rockfalls, avalanches, and landslides. Another way to predict the behavior of debris flow is to use LAHARZ [121]. LAHARZ is GIS-based software (plugin) developed by USGS (United States Geological Survey) and is used as a plugin of ArcGIS and it is written in the ArcInfo Macro language (AML) as it is described by [121].

LAHARZ is an empirical model that requires two main parameters, namely, debris flow volume and the underlying DEM (Figure 27 and Figure 28). LAHARZ was designed as a hazard-delineation tool [122] and the accuracy of the model is coarse, and it is generally used to simulate the inundation of debris flow [123]. The program assumes that the volume that leaves the proximal hazard zone (source area) equals the volume that reaches the distal hazard zone (deposition area) ([121]; [122]).

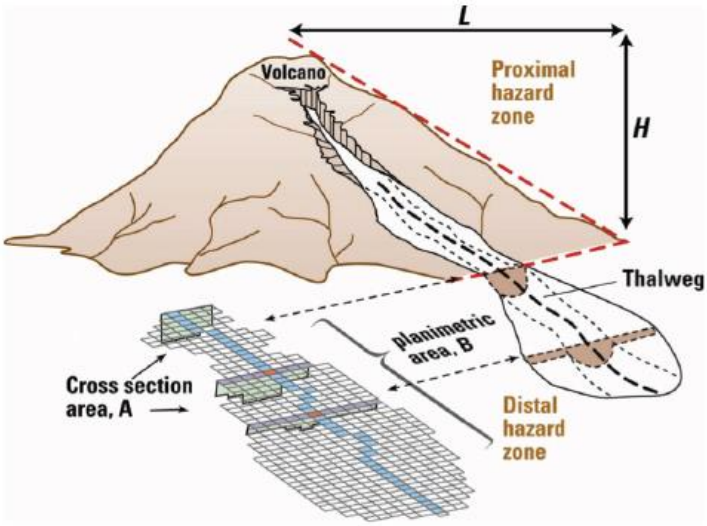

Figure 27. Diagram illustrating the planimetric area (B) and cross-sectional area (A) used by LAHARZ. The height drop (H) to horizontal runout distance (L) ratio stands for the proximal lahar hazard extent [121].

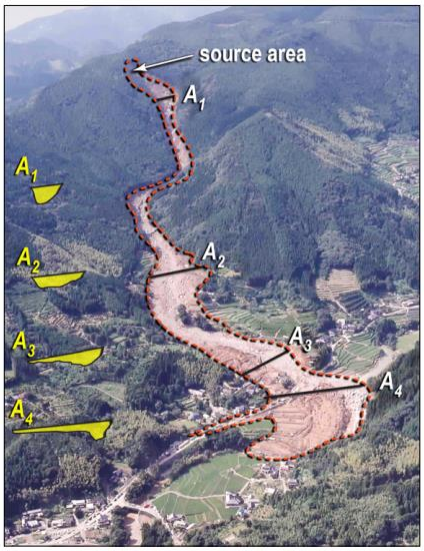

Figure 28. Diagram to illustrate Inundation extents of debris flow from source area. Cross sections areas (A) along the inundation limits are shown in yellow, whereas the total planimetric area (B) is shown by dashed lines. (July 20, 2003's Minamata debris flow in Kyushu, diagram [124]).

As discussed by Iverson et al. (1998), LAHARZ uses those to parameters to predict inundation extent (planimetric area, B) and depth in form cross-sectional area (A). [122] has predicted the relationships between volume and both cross-sectional (A) and planimetric areas (B) using scaling analysis:

$$A = c_1 V^{2/3} \tag{3.7}$$

$$B = c_2 V^{2/3} \tag{3.8}$$

Where V is the volume, A is the largest cross-sectional area through which lahar or debris pass, B is the deposition planimetric area. c1 and c2 are the proportionality coefficients. Through worldwide examination of data set, [122] has found out that c1=0.05 and c2=200 for lahars produce results closely related to observed values. This

study was expanded by [124] to examine the debris flow behavior, and it was found that for debris, c1=0.1 and c2 =20 (Figure 29).

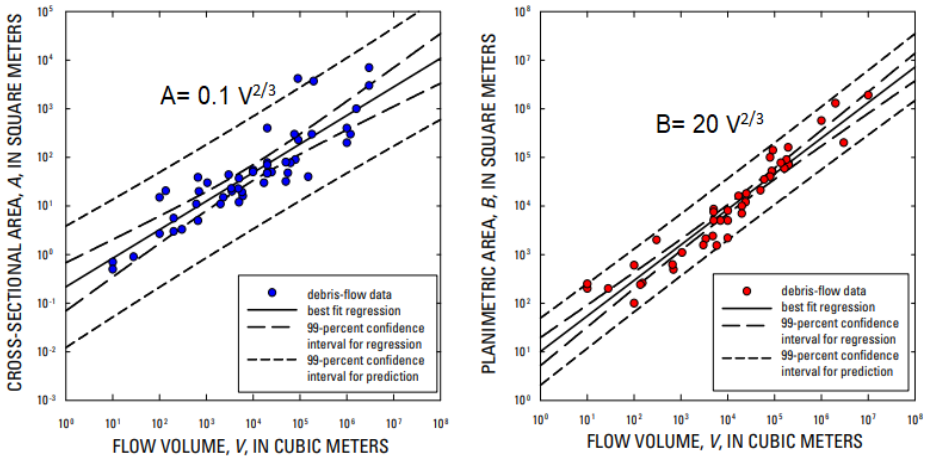

Figure 29. Relationships between volume to cross-sectional area (A) and planimetric area (B) respectively [124].

Creating debris flow inundation map in LAHARZ requires adequate topographic data (DEM), to identify potential proximal zones (source areas) and a good estimate of corresponding volumes of debris flow from each source [124]. The software has seven main tools for the analysis [122]: (i) *To Create Surface Hydrology Raster*, (ii) *Generate New Stream Network* using stream thresholds, (iii)*Create Zone Proximal* (Create a proximal hazard zone), (iv) Lahar Distal Zones (Create inundation areas based on User supplied volume), (v) Merge Rasters and (vi) *Raster to Shapefile* that converts raster to vector dataset.

3.3.1. Debris Flow Hazard Analysis

The empirical analysis of debris flow using LAHARZ starts with the preparation of a digital elevation model (DEM) of the place [125]. For our case, a 10-m resolution DEM is downloaded from the Italian territory DTM database (TINITALY) in the UTM WGS

84 zone 32 projection system as a GeoTIFF file. This DEM is also used to calculate the flow paths slopes between the transport and deposition areas (Table 4).

Another important parameter for the empirical analysis of debris flow is the volume of the mass involved. [126] has estimated each debris flow channel disrupted volume (table) by using the source area and its thickness, aerial photography, and DEM analysis. As indicated by Dorta et al. (2007), two flow categories were observed (i) those with a transport zone (Ep-1, Ep-3a, Ep-5, Ep-7a, Ep-7b, Lav-1, and Lav-2 where Ep stands for Episcopio and Lav for Lavorate) and (ii) others without transport zones (Ep-2, Ep-3b, Ep-4, Ep-6a and Ep-6b) between source and deposit areas. They have found this estimation by adding the volume of the deposited soil and the soil in the disrupted area. Recorded in the table below are the local slopes measured using the digital elevation model, peak discharge and maximum velocity values calculated using equation (3.1) and equation (3.6) respectively.

As noted above LAHARZ (GIS tools for Automated Mapping of Lahar Inundation Hazard zones) and ArcMap are free software provided by the United States Geological Survey (USGS) and can be downloaded from their website. First, we start ArcMap, and open ArcToolbox. We then load the downloaded Laharz.py.tbx to ArcToolbox. Laharz_py toolbox has seven tools as discussed in the section above. The first three are used to prepare datasets necessary for the simulation of the project. Digital elevation model is then imported into ArcMap (Figure 30) and convert it to hillshade view.

Table 4: Assessed debris flow volume and peak discharge [127], measured local slopes and estimated maximum flow velocity.

Flow	Volume (m^3)	Q (m^3s^{-1})	Slope	$V_{max}(ms^{-1})$
Ep-1	36000	600	0.34	12
Ep-2	124000	1700	0.30	16
Ep-3a	101000	1500	0.29	16
Ep-3b	88000	1300	0.40	17
Ep-4	53000	900	0.29	13
Ep-5	158000	1500	0.35	17
Ep-6a	121000	1700	0.35	17
Ep-6b	73000	1100	0.21	13
Ep-7a	38000	700	0.22	11
Ep-7b	253000	3200	0.23	19
Lav-1	105000	1600	0.28	16
Lav-2	275000	3400	0.24	19

* Where Ep stands for Episcopio and Lav for Lavorate.

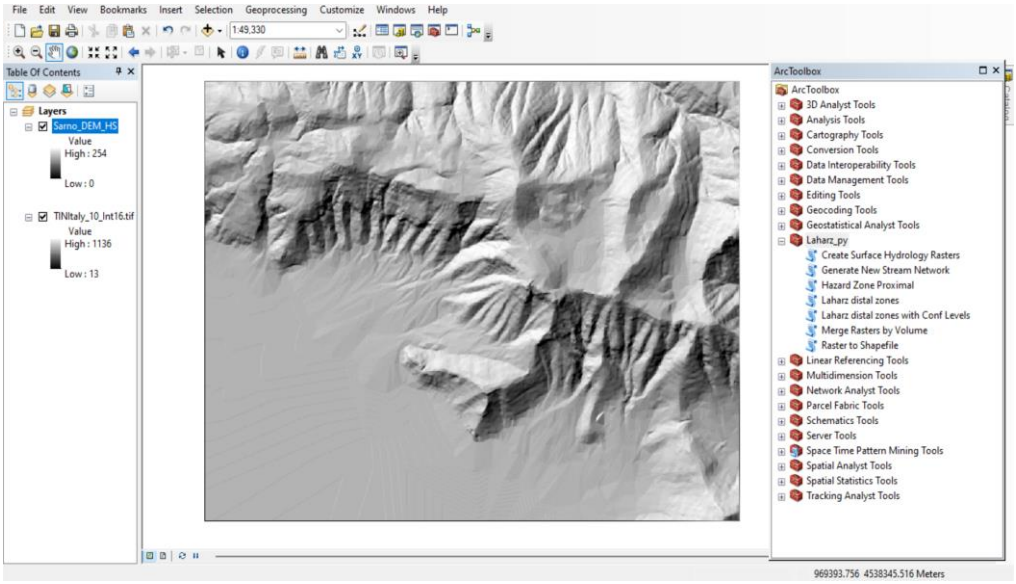

Figure 30: Hillshade view of Sarno digital elevation model in ArcMap.

As can be seen on the lists of the tools of Laharz_py [121], the simulation begins by creating surface hydrology rasters. We click on the tool, we specify our workspace and DEM, then we choose stream threshold value. When this tool is run, DEM sinks are all filled, flow accumulation, flow directions and stream raster are generated (Figure 31). This step generates four new rasters, some of which will be used in the ensuing steps. Sometimes, the user might think it expedient to regenerate another stream network with a different stream threshold value.

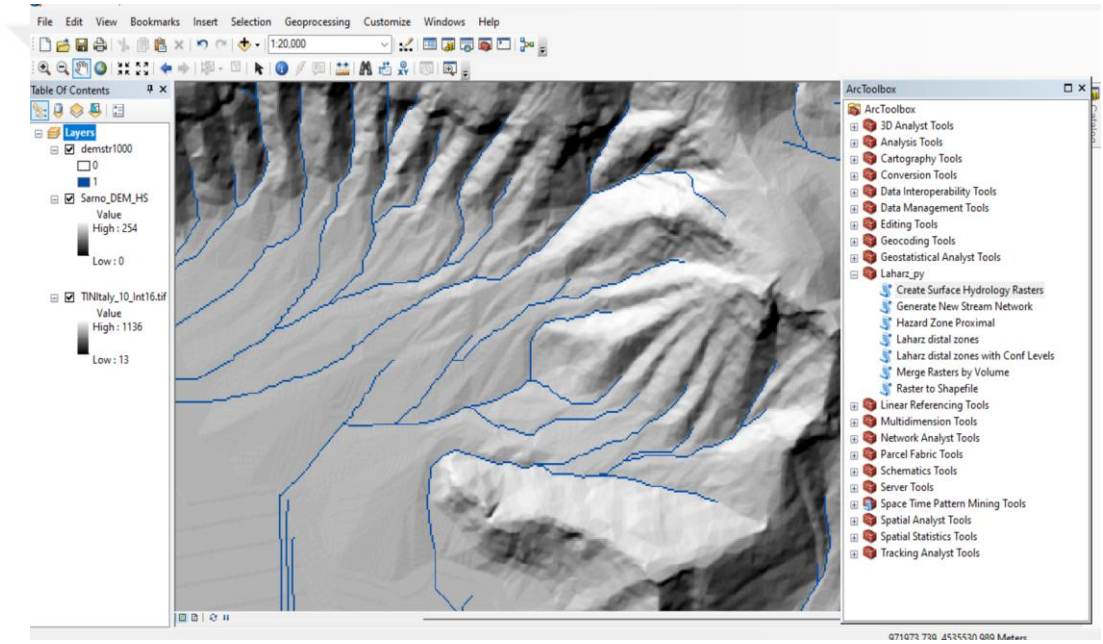

Figure 31: Created surface hydrology rasters showing Sarno stream networks.

The second step is to create proximal hazard zone boundaries using the proximal Hazard Zone boundary tool [121]. Here, we specify a filled DEM (one of the four rasters obtained above), stream raster and the slope of the cone (i.e., the height to the length ratio, H/L), and the location (XY coordinates) of the cone. Slopes used here are recorded in **Table 4** above. The Lahar Distal Zone tool is then used to calculate inundation areas of drainage whose XY coordinates are specified. In this part, volume text file containing volumes of each drainage, filled DEM, and a text file containing XY coordinates of source

area are specified. It is on this step where we specify the flow type of our simulation, namely lahar, debris_flow and Rock_Avalanche. This tool uses Equations (3.7 & (3.8) above to calculate both planimetric area and maximum cross-sectional area. When this step is completed, the program generates an inundation area file (raster file) and a text file with ". pts" file extension. The generated inundation area of each of the drainage zones can be seen in Figure 32 below.

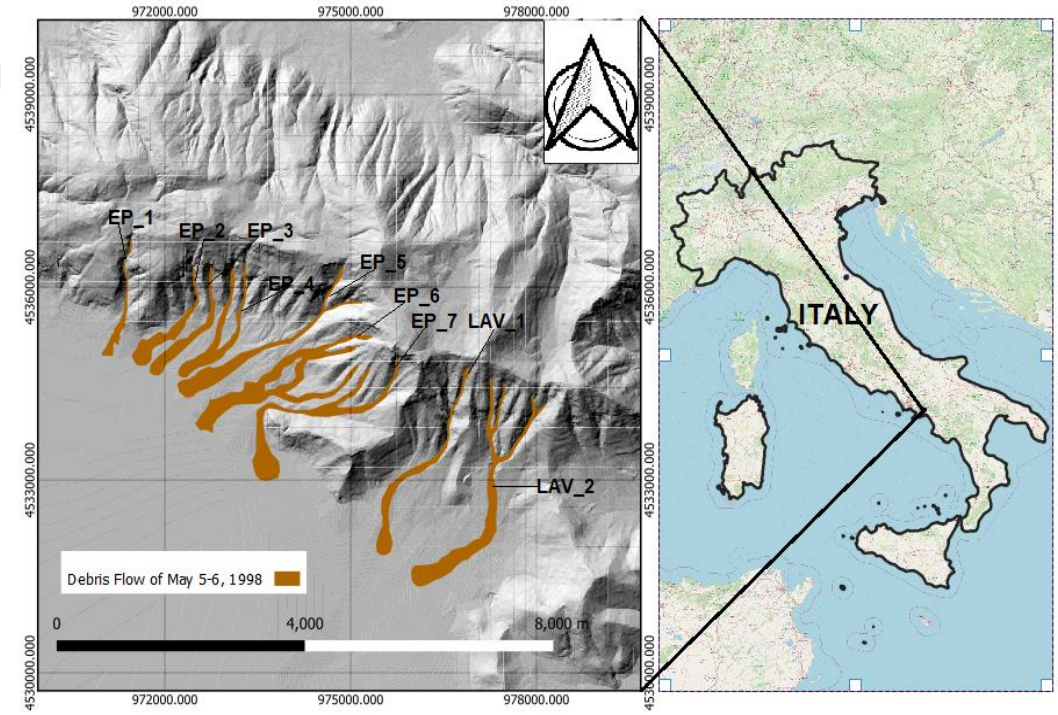

Figure 32. Generated inundation map for May 1998 Sarno debris flow in the Episcopio and Lavorate regions.

3.3.2. Exposure Analysis

Shapefiles of the building data of the Sarno region are provided Italian Government website downloaded from National dataset of Italian Structural Aggregates. However, the data available does not provide detailed information on what type of building, number of stories of the building, functions of the building and so on. According to [128] 81% of

the buildings in the Episcopio region were residential buildings, mostly masonry structures, although few reinforced structures and other framed structures were present. As for the age of the buildings, the study suggests that most of the buildings in the region were more than 30 years old at the time of the May 1998 Sarno landslides. The produced inundation map shapefiles were superimposed with the building data shapefiles to generate the May 1998 Sarno debris flow exposure map (Figure 33).

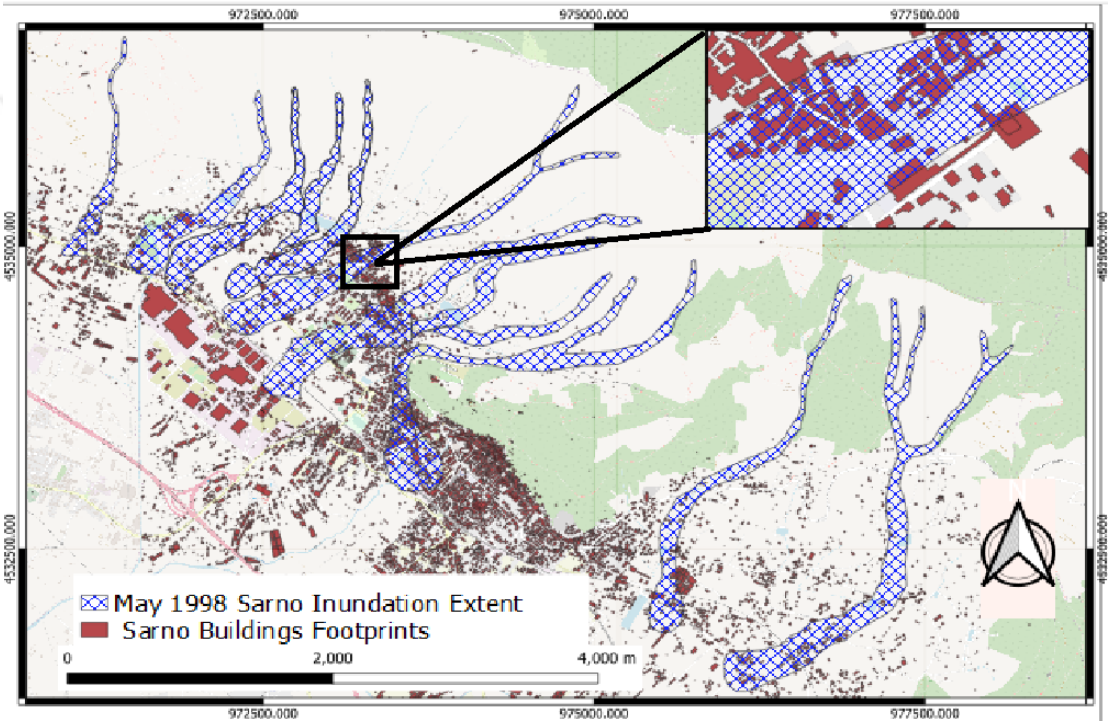

Figure 33. Generated May 05-06, 1998, Sarno debris flow hazard map

To estimate velocities affecting each individual building, 3-4 sample points were taken on each debris flow path. Cross section of each point is drawn to estimate the channel width (w) and the difference in elevation between the inner and outer bank (Δe). A circle is carefully positioned at the location of the point where velocity measurements are calculated to correctly estimate the radius of the curvature (R_c). Then using the equation (3.4), velocity is calculated. K is taken as 1 for more conservative calculations. Below is an illustrating example of velocity estimation on the Ep_7 debris flow channel.

Drawing the circle gives a circle of 370 m-diameter (185 m-radius) in Figure 34. The cross-section at the point shows a channel width of 90 meters and Δe of 0.9 meters as shown in Figure 34. Applying the Equation (3.5) gives a velocity of 18 m/s.

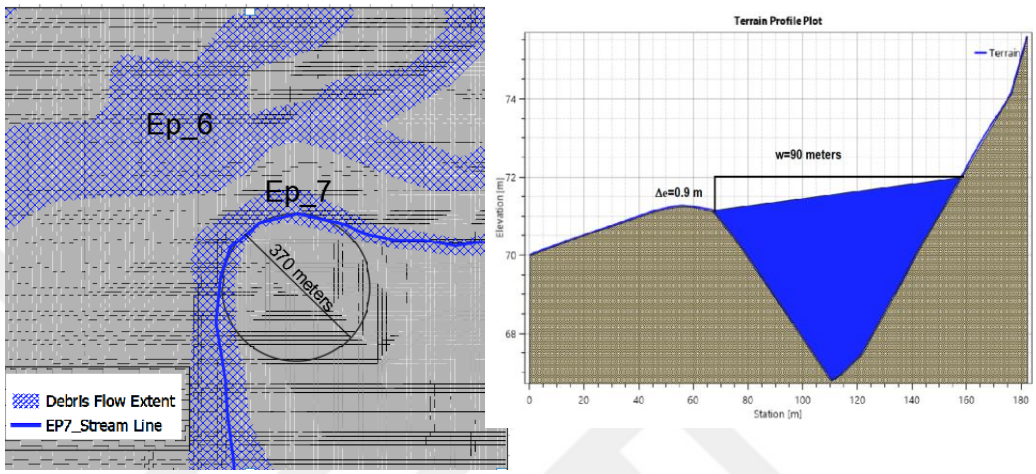

Figure 34. Diagram illustration of debris flow velocity estimation on Ep-7 channel.

3.3.3. Vulnerability Analysis

Fuchs et al. (2007) has proposed an empirical vulnerability function which has been appropriated by so many other proceeding studies in the debris flow risk assessments (Figure 35). He has appropriated well-documented data of debris flow from the Austria Alps events and has concluded that the damage pattern of masonry and concrete structures caused by debris flow can be estimated using a second order polynomial function (Equation (3.9).

$$Y = 0.11\,x^2 - 0.02\,x \tag{3.9}$$

where, y is the vulnerability second order polynomial function for all debris flow intensity, i.e., deposition height (x< 2.5 m) [34].

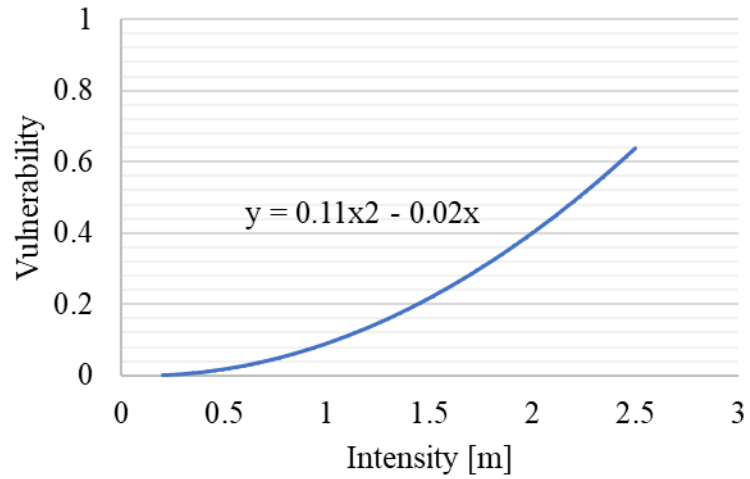

Figure 35. Fuchs et al. (2007) vulnerability curve (relationship between debris flow intensity (x) and vulnerability (y))

Another well-known study on vulnerability assessment of buildings is the work of Kang and Kim [22]. The study is based on the analysis of 11 debris flow events that took place between July and August 2011 in South Korea. Vulnerability functions based on debris flow velocity and flow depth were proposed for both reinforced concrete and non-reinforced concrete buildings as shown in Table 5, Figure 36 and Figure 37.

Table 5: Kang and Kim [35]'s vulnerability functions for building structures.

Intensity parameter	Vulnerability function	
	Non-RC frame (1)	RC frame (2)
Flow velocity [v (m/s)]	$V = 1 - e^{(-0.0140 \times v^{4.368})}$	$V = 1 - e^{(-0.0094 \times v^{2.775})}$
Flow depth [d (m)]	$V = 1 - e^{(-2.2072 \times d^{2.019})}$	$V = 1 - e^{(-0.1703 \times d^{1.537})}$
Impact pressure [P (kPa)]	$V = 1 - e^{(-0.0010 \times p^{2.227})}$	$V = 1 - e^{(-0.0005 \times p^{1.690})}$

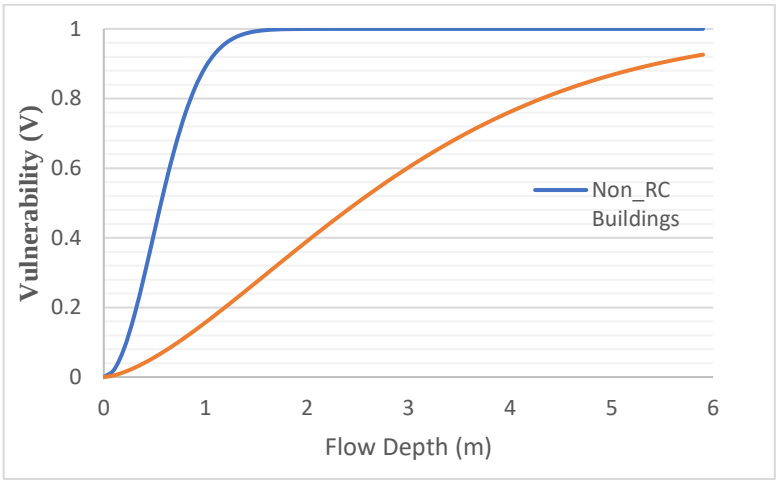

Figure 36. Kang and Kim [22]'s debris flow vulnerability curves as a function of flow depth.

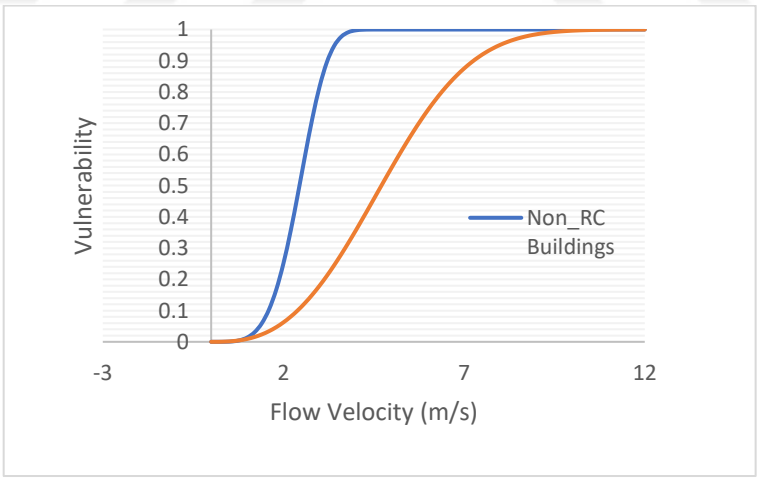

Figure 37. Kang and Kim [22]'s debris flow vulnerability curves as a function of flow velocity.

We have also used the empirical vulnerability functions suggested by [36]. Those functions were developed following the July 13, 2008, debris, and mud flow in the central parts of Valtellina between Berbenno and Morbegno, Selvetta Province of Italy. The

study suggests a second order polynomial relationship between debris deposition height and the building vulnerability (see Figure 38). The function is used for both masonry and reinforced concrete single to four-story buildings.

$$V = 0.17\,h^{2} - 0.03\,h \tag{3.10}$$

where V is the vulnerability function and h are the deposition height of debris flow with values between 0 and 2.5 m.

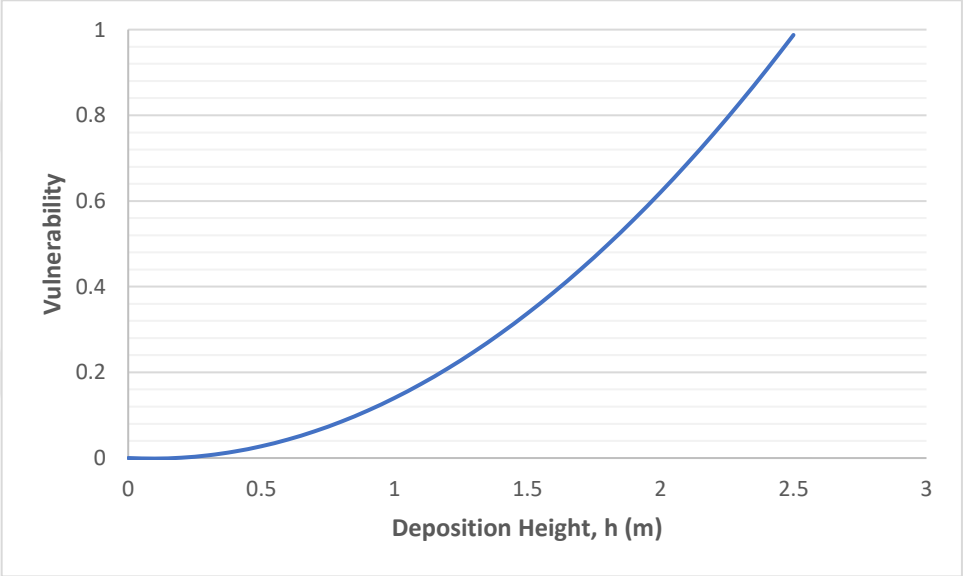

Figure 38. Akbas et al. [36] vulnerability curve.

To estimate the losses, buildings in the debris flow extent were identified, then using linear interpolation, debris flow velocities and depth on each building was estimated. Using the above discussed methods, namely Fuchs [34], Kang and Kim [35], and Akbas [36], building damages due to debris flow in the Sarno region were calculated. To estimate the economic losses on each building, we have adopted the Huizinga et al. (2017) building-based and content damage values for residential buildings in Italy. [29] estimates a total of €739 per square meter. Figure 39 below shows estimated total

financial loss using the three debris flow damage functions. Fuchs, Kang and Kim, and Akbas debris flow damage functions estimate € 93 million, € 167 million, and €102 million of financial losses respectively. The damage costs estimated by both Fuchs and Akbas are comparatively low compared to the damage estimated by Kang and Kim functions. This is fundamentally due to the type of damage functions used in those studies as Fuchs and Akbas both propose second order polynomial function whereas Kang and Kim use exponential function to estimate the damage costs.

It is hard to clearly validate the estimations done here since there is no detailed study of economic losses of the May 1998 Sarno debris flow event. Nevertheless, [11] estimates $100 million property losses of the May 1998 Sarno debris flow. This amount agrees with the damage costs estimated using both Fuchs and Akbas methods. It is also important to add that the Akbas debris flow damage functions were developed following the July 13, 2008, debris, and mud flow in the central parts of Valtellina between Berbenno and Morbegno, Selvetta Province of Italy, which explains why it might be the most correct estimation.

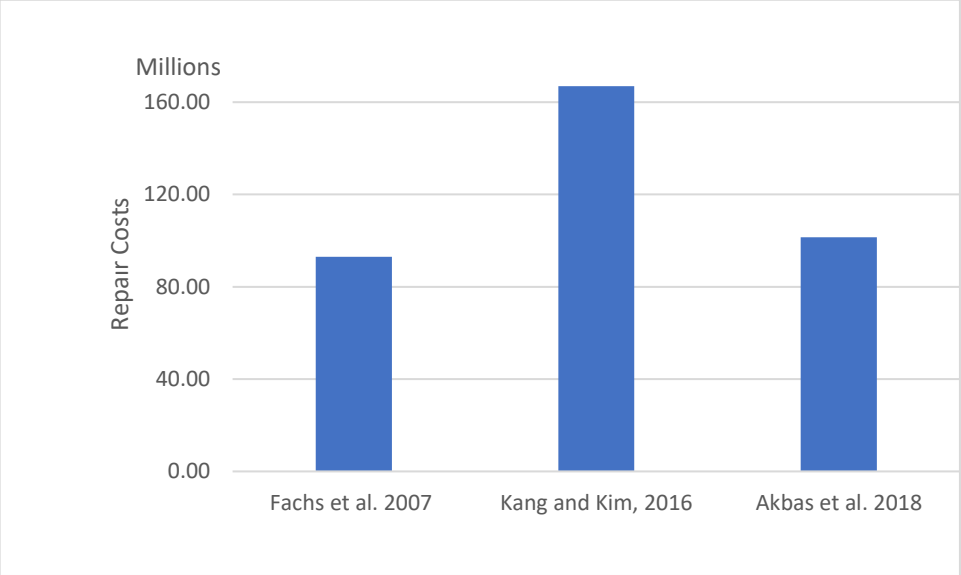

Figure 39. Diagram comparing the total estimated building losses due to May 5-6, 1998, Sarno debris flow.

Additionally, uncertainties associated with unit prices and building properties and the impact of these uncertainties on the loss quantities are evaluated. The spatial correlations in demand and capacity of buildings to withstand the hazard are incorporated to assess the overall loss estimation for a particular region. Here Equations (2.11), (2.12)& (2.13) from [63], are used. Figure 40 demonstrates the probability of exceedance for the aggregated debris flow losses using the three different methods used above, Fuchs, Kang and Kim and Akbas methods. From Figure 40, it can be concluded that not accounting for spatial correlation in losses resulting from shared hazard exposure and building vulnerability can lead to an underestimation of the comprehensive loss and recovery evaluations for the highest levels of loss occurrences.

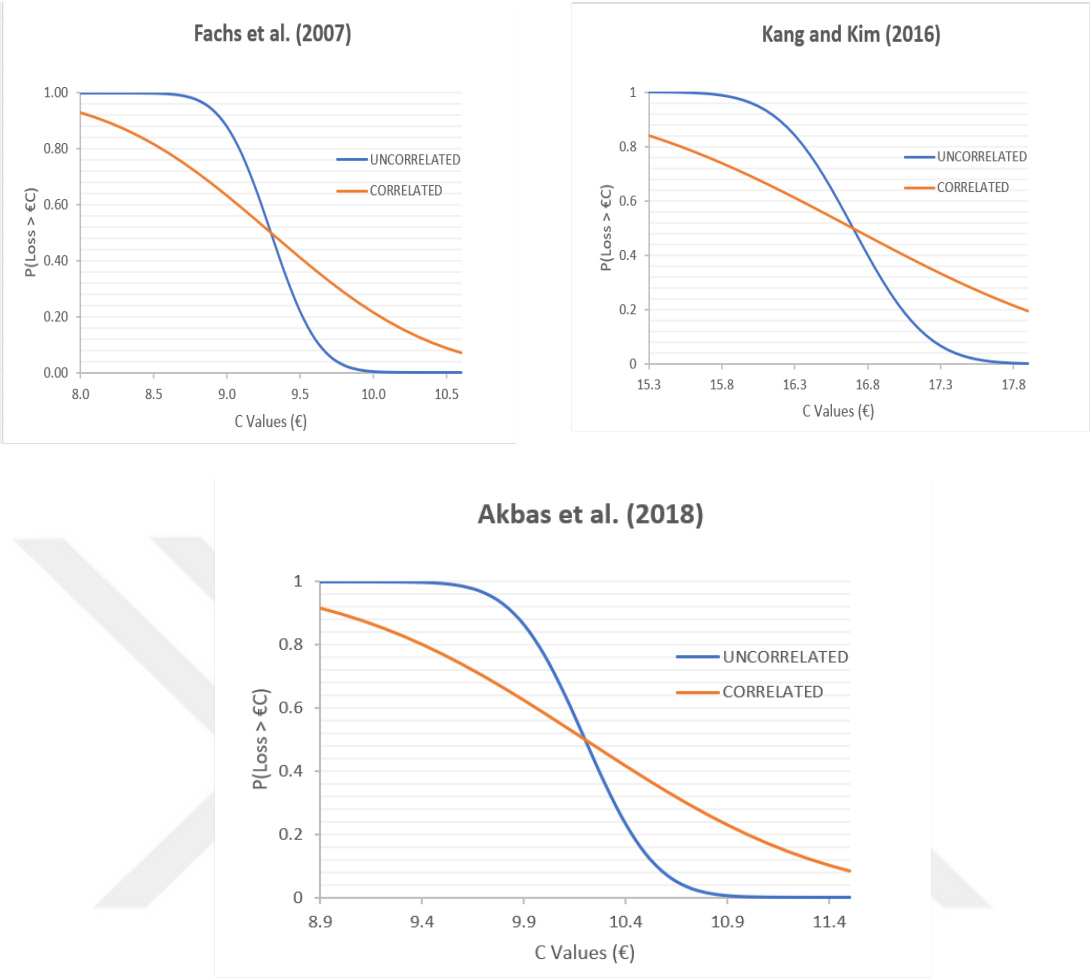

Figure 40. Probability of exceedance for the aggregated Debris flow losses.

3.4. Sensitivity Analysis

The main obstacle in the process of debris flow loss estimations lies in the calculation of debris flow velocity. Debris flow velocity calculation is a rigorous process that might not be practical. Hence, we have opted to use maximum velocity and calculated the maximum expected financial loss from a debris flow hazard. Using the maximum velocity in each of the flow channels of the 1998 Sarno debris flow hazard, the estimated loss changes from €167 million to €223 million using Kang and Kim loss method.

We have also examined how the total loss would be by changing the debris volume (V). We have calculated the total financial loss by using twice the volume (2V),

half of the volume (0.5V) and a quarter of the volume (0.25V) in each channel source. Table 6 below shows the results of the analysis. Doubling the debris flow volume would result in a total financial loss of €386 million while halving the debris volume would cause a loss of €129 million based on Kang and Kim's loss method.

Table 6: Results of debris flow loss assessment using different debris flow volumes.

Volume Input (m^3)	Debris Flow Loss (€ million)
Twice the Volume (2V)	386
Actual Volume (V)	223
Half the Volume (0.5)	129
Quarter the Volume (0.25V)	74

Due to limited availability of data for the case of Sarno debris flow, the relationship between debris flow intensity (which is debris flow volume for this case study) cannot be suggested. However, from the few data in Table 6 above it can be inferred that there is a relationship between the debris flow volume and the regional loss for the Sarno region.

CHAPTER IV

CONCLUSION

4.1. Summary

This study was done on two rainfall triggered natural disasters: flooding and debris flow. The world suffers greatly from those two natural hazards and Turkey is not an exception. Given the sheer effects of the two hazards, our study aims at contributing to the development of proper and practical methods for the hazards' risk assessment and management. Moreover, having realized the research gap on the consideration of flood and debris flow plagued uncertainties, the study shades light on the effects of ignoring uncertainties and spatial correlation on the total regional flood losses.

First, using the flood hazard and loss assessment framework found in the literature, a regional flood hazard modelling is performed on the town of Bozkurt in Turkey. A hydrologic analysis is performed using HEC-HMS, a hydraulic analysis using HEC-RAS, an exposure analysis is done in QGIS program, and a vulnerability analysis is performed using four different methods of flood financial loss estimation on individual building losses. Additionally, we have investigated the effects of uncertainties and spatial correlations to the overall regional flood loss costs. From the analysis, it can be inferred that it is unconservative to ignore the uncertainties during hazard loss assessment. It should also be added that the study does not seek to quantify uncertainties related to flood loss, therefore, a reasonable coefficient of variation of 0.3 was chosen to represent individual building's inherent uncertainties. As discussed above, a sensitivity analysis is performed using flood discharge as the only variable. The suggested relationships between flood discharge to flood loss are only representative of the loss of Bozkurt.

Second, the study performs a debris flow and loss analysis. Using the May 1998 Sarno debris flow in Italy as a case study, the debris flow of the place is modeled in Laharz software. Exposure analysis is also done on the buildings in the affected region and corresponding direct building costs are estimated. As is the case for all natural disasters, debris flow modeling also is not free of uncertainties and the study investigates the effect of including uncertainties and spatial correlation on the total costs. It is realized that ignoring them can lead to wrong loss estimates, especially for extreme events. Sensitivity analysis is performed for some values of debris flow volume on the area. Due to complex nature analysis and difficulties in calculating the needed debris flow intensities, the study has not established the relationship between flow volume and incurred losses.

4.2. Limitations and Future Works

Although the study is intended to contribute to literature in the field of hazard loss modeling, some assumptions were made due to the following limitations:

- There is a lack of flood and debris flow damage curves that are specific to Turkey. For this reason, the used damage curves are borrowed from other studies in literature.
- There is a lack or limited knowledge of the uncertainties inherent to flood and debris flow hazard modeling and loss assessment.
- As shown, the amount of structural damage incurred by natural disasters is a combination of many factors like the function of the building, the age of the building, the building material of the building and the number of stories of the considered building. Limited information on the above-mentioned building aspects can lead to wrong and unconservative loss estimates.

- The study also uses full replacement costs provided by Huizinga et al. (2017) rather than depreciated buildings values.
- There is a lack of enough data to validate the hydrological and hydraulic models.
- The study uses a relatively low-resolution DEM, thus fails to capture detailed information of basin and stream channels. For that reason, there is limited data on the physical characteristics of the places studied.
- There is a lack of debris flow data of the past events in Turkey. This is somewhat problematic since it shows that despite the past recorded landslides, little has been done to enhance the data on landslides in the country.
- Due to the complex nature and limited knowledge on the flow mechanism of debris flow, it is difficult to quantify its velocity and other flow parameters, especially in the absence of observed data.

Below are the suggested future works and related parties should be engaged in finding the necessary solutions:

- The flood study only covers the town of Bozkurt whereas it is expedient that such readily available models can be done on all water basins, or at least flood-prone regions in Turkey.
- Given the need of flood and debris flow damage curves for buildings, further research is needed to develop those curves that would ease the estimation of the hazard's loss.
- Development of comprehensive building database is needed for all towns in Turkey and should be made readily accessible to researchers in the corresponding areas.
- Further studies should be conducted to understand fully the mechanism of debris flow.
- Effort should be directed in the proper quantification of hazard related uncertainties.

REFERENCES

[1] A.A. Sadiq, J. Tyler, & D.S. Noonan. “A review of community flood risk management studies in the United States”. *International Journal of Disaster Risk Reduction*, vol. *41*, p. 101327,2019.

[2] G. Koç, T. Petrow, & A.H. Thieken. “Analysis of the most severe flood events in Turkey (1960–2014): which triggering mechanisms and aggravating pathways can be identified? *Water*, vol. *12*(6), p. 1562, 2020”.

[3] M. K. Kelesoglu, R. Temur, S. Gülbaz, N.M. Apaydin, C.M. Kazezyılmaz-Alhan, & I. Bozbey, I. “Site Assessment and Evaluation of the Structural Damages After the Flood Disaster in the Western Black Sea Basin on August 11, 2021”, *Natural hazards*, vol. 116, pp. 587-618.

[4] C. Dandridge, T.A. Stanley, D.B. Kirschbaum, & V. Lakshmi. “Spatial and Temporal Analysis of Global Landslide Reporting Using a Decade of the Global Landslide Catalog”. *Sustainability*, vol. *15*(4), p. 3323, 2023.

[5] P.J. Ward, V. Blauhut, N. Bloemendaal, J.E. Daniell, M.C. de Ruiter, M.J. Duncan, ... & H.C. Winsemius. “Natural hazard risk assessments at the global scale”. *Natural Hazards and Earth System Sciences*, vol. *20*(4), pp. 1069-1096, 2020.

[6] T. Çan, T.Y. Duman, S. Olgun, S. Çörekçioğlu, F. Karakaya-Gülmez, H. Elmacı, ... & O. Emre. “Türkiye Heyelan Veri Tabani.” *TMMOB Coğrafi Bilgi Sistemleri Kongresi, Ankara, 2013”*.

[7] T.Y. Duman, T. Çan,, O Emre, M. Keçer, A. Doğan, S. Ateş & Durmaz. “Landslide inventory of northwestern Anatolia, Turkey”. *Engineering geology*, vol. *77*(1-2), pp. 99-114, 2005.

[8] M. Ahmadi-Adli. “Shallow landslides triggered by rainfall in unsaturated soils”, PhD. Thesis, civil engineering, METU, Ankara, Turkey, 2014.

[9] B. Ildır. “Türkiye’de heyelanların dağılımı ve afetler yasası ile ilgili uygulamalar”. In *2nd National Landslide Symposium, Sakarya, Türkiye, Eylül*. 1995, pp. 1-9.

[10] T. Görüm & S. Fidan. “Spatiotemporal variations of fatal landslides in Turkey”. *Landslides*, vol. *18*(5), pp. 1691-1705, 2021.

[11] D. Calcaterra, M. Parise, B. Palma & L. Pelella. “Multiple debris-flows in volcaniclastic materials mantling carbonate slopes”. In *Debris-flow hazards mitigation: mechanics, prediction, and assessment, vol. 1*, pp. 99-107, 2000.

[12] M. Jakob, D. Stein, & M. Ulmi. “The vulnerability of buildings to debris flow impact”. *Natural hazards*, vol. *60*, pp. 241-261, 2012.

[13] G. Capparelli, & P. Versace. “Analysis of landslide triggering conditions in the Sarno area using a physically based model”. *Hydrology and Earth System Sciences*, vol. 18(8), pp. 3225-3237, 2014.

[14] M. Calvello, M. N. Papa, J. Pratschke, & M. Nacchia Crescenzo. “Landslide risk perception: a case study in Southern Italy”. *Landslides*, vol.13, pp. 349-360, 2016.

[15] G. Toyos, R. Gunasekera, G. Zanchetta, C. Oppenheimer, R. Sulpizio, M. Favalli, & M. T. Pareschi. “GIS-assisted modelling for debris flow hazard assessment based on the events of May 1998 in the area of Sarno, Southern Italy: II”. Velocity and dynamic pressure. Earth Surface Processes and Landforms: *The Journal of the British Geomorphological Research Group*, vol. 33(11), pp. 1693-1708, 2008.

[16] J. M. Wright. “Floodplain management: Principles and current practices”. Ph.D. thesis, Civ Eng., *Knoxville: The University of Tennessee, 2008*.

[17] Y. B. Liu, F. De Smedt, L. Hoffmann & L. Pfister. “Assessing land use impacts on flood processes in complex terrain by using GIS and modeling approach”. *Environmental modeling & assessment*, vol. *9*, pp. 227-235, 2005.

[18] S. Gülbaz & C. M. Kazezyılmaz-Alhan. “Calibrated hydrodynamic model for Sazlıdere watershed in Istanbul and investigation of urbanization effects”. *Journal of Hydrologic Engineering*, vol. *18*(1), pp. 75-84, 2013.

[19] Tsakiris, G. J. N. H. (2014). “Flood risk assessment: concepts, modelling, applications”. *Natural Hazards and Earth System Sciences*, vol. *14*(5), pp. 1361-1369, 2014.

[20] W. Kron. “Flood risk hazard values vulnerability”. *Water Int*, vol. *30*(1), pp. 58-68, 2005.

[21] O. M. Nofal & J. W. van de Lindt. “Probabilistic flood loss assessment at the community scale: A case study of 2016 flooding in Lumberton, North Carolina”. *ASCE-ASME Journal of Risk and Uncertainty in Engineering Systems, Part A: Civil Engineering*, vol. *6*(2), p. 05020001, 2020.

[22] B. Merz, H. Kreibich, A. Thieken & R. chmidtke. “Estimation uncertainty of direct monetary flood damage to buildings”. *Natural Hazards and Earth System Sciences*, vol. *4*(1), pp. 153-163, 2004.

[23] M. T. Marvi. “A review of flood damage analysis for a building structure and contents”. *Natural Hazards*, vol. *102*(3), pp. 967-995, 2020.

[24] O. D. Aribisala, S. G. Yum, M. D. Adhikari & M. S. Song. “Flood Damage Assessment: A Review of Microscale Methodologies for Residential Buildings”. *Sustainability*, vol. *14*(21), p. 13817, 2022.

[25] E. Penning-Rowsell, C. Johnson, S. Tunstall, S. Tapsell, J. Morris, J. Chatterton & C. Green. “The benefits of flood and coastal risk management: a handbook of assessment techniques”. *ISBN 1904750516, 2005*.

[26] H. Kreibich & A. H. Thieken. “Assessment of damage caused by high groundwater inundation”. *Water Resources Research*, vol. *44*(9), pp. 108-122 2008.

[27] F. Messner & V. Meyer. “Flood damage, vulnerability and risk perception–challenges for flood damage research”. In *Flood risk management: hazards, vulnerability and mitigation measures* vol. 6, pp. 149-167, 2006.

[28] E. Genovese. “A methodological approach to land use-based flood damage assessment in urban areas: Prague case study”. *Technical EUR Reports, EUR, 22497, 2006*.

[29] J. Huizinga, H. De Moel, & W. Szewczyk. “Global flood depth-damage functions: Methodology and the database with guidelines” (No. JRC105688). Joint Research Centre (Seville site), 2017.

[30] A. K. Pistrika, & S.N Jonkman. “Damage to residential buildings due to flooding of New Orleans after Hurricane Katrina”. *Natural Hazards*, vol. *54*, pp. 413-434, 2010.

[31] H. Maiwald, & J. Schwarz. “Damage and loss prognosis tools correlating flood action and building’s resistance-type parameters”. *International Journal of Safety and Security Engineering*, vol. *5*(3), pp. 222-250, 2015.

[32] H. Maiwald, J. Schwarz, C. Kaufmann, T. Langhammer, S. Golz, & T. Wehner. “Innovative vulnerability and risk assessment of urban areas against flood events: prognosis of structural damage with a new approach considering flow velocity”. *Water*, vol. *14*(18), p. 2793, 2022.

[33] https://www.usgs.gov/software/laharz

[34] S. Fuchs, K. Heiss, & J. Hübl. “Towards an empirical vulnerability function for use in debris flow risk assessment”. *Natural Hazards and Earth System Sciences*, vol. *7*(5), pp. 495-506, 2007.

[35] H. S. Kang & Y. T. Kim. “The physical vulnerability of different types of building structure to debris flow events”. *Natural Hazards*, vol. *80*, pp. 1475-1493, 2016.

[36] S. O. Akbas, J. Blahut & S. Sterlacchini. “Critical assessment of existing physical vulnerability estimation approaches for debris flows”. *Landslide processes: from geomorphological mapping to dynamic modelling*, pp. 229-233, 2009.

[37] B. Jongman, H. Kreibich, H. Apel, J.I. Barredo, P.D. Bates, L. Feyen, & P. J. Ward. “Comparative flood damage model assessment: towards a European approach”. *Natural Hazards and Earth System Sciences*, vol. *12*(12), pp. 3733-3752, 2012.

[38] S. Menoni, D. Molinari, F. Ballio, G. Minucci, O. Mejri, F. Atun & C. Pandolfo. “Flood damage: a model for consistent, complete and multipurpose scenarios”. *Natural Hazards and Earth System Sciences*, vol. *16*(12), pp. 2783-2797, 2016.

[39] J. Hall & M. Anderson. “Handling uncertainty in extreme or unrepeatable hydrological processes—the need for an alternative paradigm”. *Hydrological Processes*, vol. *16*(9), pp. 1867-1870, 2002.

[40] L. Wouters, A. Couasnon, M. C. De Ruiter, M. J. Van Den Homberg, A. Teklesadik & H. De Moel. “Improving flood damage assessments in data-scarce areas by retrieval of building characteristics through UAV image segmentation and machine learning–a case study of the 2019 floods in southern Malawi”. *Natural Hazards and Earth System Sciences*, vol. *21*(10), pp. 3199-3218, 2021.

[41] B. B. Shrestha, A. Kawasaki, & W. W. Zin. “Development of flood damage assessment method for residential areas considering various house types for Bago Region of Myanmar”. *International Journal of Disaster Risk Reduction*, vol. *66*, p. 102602, 2021.

[42] A. Zerger. “Examining GIS decision utility for natural hazard risk modelling”. *Environmental modelling & software*, vol. *17*(3), pp. 287-294, 2002.

[43] H. Apel, B. Merz & A. H. Thieken. “Quantification of uncertainties in flood risk assessments”. *International Journal of River Basin Management*, vol. *6*(2), pp. 149-162, 2008.

[44] K. H. Hu, P. Cui & J. Q. Zhang. “Characteristics of damage to buildings by debris flows on 7 August 2010 in Zhouqu, Western China”. *Natural Hazards and Earth System Sciences*, vol. *12*(7), pp. 2209-2217, 2012.

[45] F. Nadim & O. Kjekstad. “Assessment of global high-risk landslide disaster hotspots”. In *Landslides–disaster risk reduction* pp. 213-221. Berlin, Heidelberg: Springer Berlin Heidelberg, 2009.

[46] C. J. Van Westen, N. Rengers & R. Soeters. “Use of geomorphological information in indirect landslide susceptibility assessment”. *Natural hazards*, vol.*30*, pp. 399-419, 2003.

[47] R. M. Iverson. “The physics of debris flows”. *Reviews of geophysics*, vol. *35*(3), pp. 245-296, 1997.

[48] M. Papathoma-Koehle, M. Keiler, R. Totschnig & T. Glade. “Improvement of vulnerability curves using data from extreme events: debris flow event in South Tyrol”. *Natural Hazards*, vol. *64*, pp. 2083-2105, 2012.

[49] M. Papathoma-Köhle, A. Zischg, S. Fuchs, T. Glade & M. Keiler. “Loss estimation for landslides in mountain areas–An integrated toolbox for vulnerability assessment and damage documentation”. *Environmental Modelling & Software*, vol. *63*, pp. 156-169, 2015.

[50] R. Totschnig & S. Fuchs. “Mountain torrents: quantifying vulnerability and assessing uncertainties”. *Engineering Geology*, vol. *155*, pp. 31-44, 2013.

[51] R. Fell, K. K. Ho, S. Lacasse & E. Leroi. “A framework for landslide risk assessment and management”. *Landslide risk management*, vol. 1, pp. 3-25, 2005.

[52] J. Blahut, T. Glade & S. Sterlacchini. “Debris flows risk analysis and direct loss estimation: the case study of Valtellina di Tirano, Italy”. *Journal of Mountain Science*, vol. *11*, pp. 288-307, 2014.

[53] J. Remondo, J. Bonachea & A. Cendrero. “Quantitative landslide risk assessment and mapping on the basis of recenT occurrences”. *Geomorphology*, vol. *94*(3-4), pp. 496-507. 2008.

[54] M. Silva & S. Pereira. “Assessment of physical vulnerability and potential losses of buildings due to shallow slides”. *Natural Hazards*, vol. *72*, pp. 1029-1050, 2014.

[55] B. Quan Luna, J. Blahut, C. Camera, C. van Westen, T. Apuani, V. Jetten & Sterlacchini. “Physically based dynamic run-out modelling for quantitative debris flow risk assessment: a case study in Tresenda, northern Italy”. *Environmental Earth Sciences*, vol. *72*, pp. 645-661, 2014.

[56] J. Corominas, C. van Westen, P. Frattini, L. Cascini, J. P. Malet, S. Fotopoulou & J. T. Smith. “Recommendations for the quantitative analysis of landslide risk”. *Bulletin of engineering geology and the environment*, vol. *73*, pp. 209-263, 2014.

[57] M. Cardinali, P. Reichenbach, F. Guzzetti, F. Ardizzone, G. Antonini, M. Galli & P. Salvati. “A geomorphological approach to the estimation of landslide hazards and risks in Umbria, Central Italy”. *Natural Hazards and Earth System Sciences*, vol. *2*, pp. 57-72, 2002.

[58] C. J. Van Westen, T. W. Van Asch & R. Soeters. “Landslide hazard and risk zonation—why is it still so difficult?” *Bulletin of Engineering geology and the Environment*, vol. *65*, pp. 167-184, 2006.

[59] R. L. Ciurean, H. Hussin, C. J. Van Westen, M. Jaboyedoff, P. Nicolet, L. Chen, S. Frigerio, and T. Glade. "Multi-scale debris flow vulnerability assessment and direct loss estimation of buildings in the Eastern Italian Alps." *Natural hazards* vol. 85, pp. 929-957, 2017.

[60] H. de MOEL & J. C. Aerts. “Effect of uncertainty in land use, damage models and inundation depth on flood damage estimates”. *Natural Hazards*, vol. *58*, pp. 407-425, 2011.

[61] H. Apel, B. Merz & A. H. Thieken. “Quantification of uncertainties in flood risk assessments”. *International Journal of River Basin Management*, vol. *6*(2), pp. 149-162, 2008.

[62] B. Merz & A. H. Thieken. “Flood risk curves and uncertainty bounds”. *Natural hazards*, vol. *51*, pp. 437-458, 2009.

[63] D. Deniz, E. E. Arneson, A. B. Liel, S. Dashti & A. N. Javernick-Will. ‘Flood loss models for residential buildings, based on the 2013 Colorado floods”. *Natural Hazards*, vol. *85*(2), pp. 977-1003, 2017.

[64] G. Bilgen, E. Balci & M. Y. Kalça. "Kastamonu Bozkurt ilçesinde 11.08. 2021 tarihinde meydana gelen sel felaketinin yerinde incelenmesi." *Tasarım Mimarlık ve Mühendislik Dergisi*, vol. *2*(1), pp. 20-35, 2021.

[65] https://www.sanalsantiye.com/kastamonu-bozkurtta-meydana-gelen-taskinin-sebebi/

[66] https://ankara.imo.org.tr/TR,48128/11-agustos-2021-bozkurt-taskin-felaketi-degerlendirme-raporu-yayimlandi.html

[67] https://www.hec.usace.army.mil/confluence/hmsdocs/hmsum/latest

[68] A. Deniz, A.D. Sahin, T. Azime, I. Dabanli. "Bozkurt Sel Afeti Sebepler ve tesipler." Civil Engineering, Istanbul Technical University, Istanbul, Turkiye, Technical Report, [Online] available: https://haberler.itu.edu.tr/docs/default-source/default-document-library/bozkurt-rapor_final.pdf?sfvrsn=fac1b83a_2, 2021.

[69] G. W. Brunner. HEC-RAS River Analysis System: Hydraulic Reference Manual, Version 5.0. *US Army Corps of Engineers–Hydrologic Engineering Center*, vol. 5, p. *547, 2016*.

[70] Karaguzel Remzi, Gülçin Türkkan Karaoğlu, Koray K. Yılmaz, Burak Çatlıoğlu, Tolga Çan, Semih Sami Akay. "Kastamonu-Bozkurt 11 Ağustos 2021 Taşkını. 2021." Yer Muhendisligi, Ankara, Turkiye Available: http://muhjeoder.org.tr/Gorsel/muhjeoder_12fb71c0ddd83ade33ac6329629024ff.PDF

[71] H. Baycan, M. Ciner, C. Gök, I. Peker & S. Gülbaz. "Flood modeling of ezine and Ayancik stream watersheds in western black sea basin, turkey.", *14th of the International Conference on Hydroscience & Engineering*, ICHE 2022

[72] A. Caglayan, R. Saber & V. Isik. 'Assessment of August 11, 2021,Bozkurt Flood Disaster With Sentinel-2 Satellite Images, Turkey". In *11th Congress of the Balkan Geophysical Society*, Vol. 2021, No. 1, pp. 1-5. EAGE Publications BV, 2021.

[73] G. R. Puno, R. C. C. Puno & I. V. Maghuyop. "Flood hazard simulation and mapping using digital elevation models with different resolutions". *Global Journal of Environmental Science and Management*, vol. *8*(3), pp. 339-352, 2022.

[74] https://docs.qgis.org/3.28/en/docs/user_manual/index.html

[75] https://earth.google.com/web/

[76] https://www.openstreetmap.org/

[77] O. D. Aribisala, S. G. Yum, M. D. Adhikari & M. S. Song. "Flood Damage Assessment: A Review of Microscale Methodologies for Residential Buildings". *Sustainability*, vol. *14*(21), p. 13817, 2022.

[78] I.K. Menteşe & N. Eroğlu. "Kastamonu Bozkurt Ezine Çayi Havza Parametrelerinin Arcgis-Hydrology İle Belirlenmesi ve Taşkin Debilerinin Hesaplanması." In *The 14th International Scientific Research Congress*, p. 15, 2022.

[79] B. Merz, H. Kreibich, A. Thieken & R. Schmidtke. "Estimation uncertainty of direct monetary flood damage to buildings". *Natural Hazards and Earth System Sciences*, vol. *4*(1), pp. 153-163, 2004.

[80] R. Huang & X. Fan. "The landslide story". *Nature Geoscience*, vol. *6*(5), pp. 325-326, 2013.

[81] R. Sidle & H. Ochiai. "Processes, prediction, and land use". *Water resources monograph. American Geophysical Union, Washington*, vol. 13, p. *525, 2006*.

[82] M. Parise. "Landslide mapping techniques and their use in the assessment of the landslide hazard". *Physics and Chemistry of the Earth, Part C: Solar, Terrestrial & Planetary Science*, vol. *26*(9), pp. 697-703, 2001.

[83] F. Guzzetti, A. C. Mondini, M. Cardinali, F. Fiorucci, M. Santangelo & K. T. Chang. "Landslide inventory maps: new tools for an old problem". *Earth-Science Reviews*, vol. *112*(1-2), pp. 42-66, 2012.

[84] H. Luo, L. Zhang, H. Wang & J. He. "Multi-hazard vulnerability of buildings to debris flows". *Engineering Geology*, vol. *279*, pp. 105859, 2020.

[85] J. L. Zêzere, R. A. C. Garcia, S. C. Oliveira & E. Reis. "Probabilistic landslide risk analysis considering direct costs in the area north of Lisbon (Portugal)". *Geomorphology*, vol.*94*(3-4), pp. 467-495, 2008.

[86] D. Crudden. "A simple definition of a landslide". *Bulletin of Engineering Geology & the Environment*, vol. *43*(1), pp. 27-29, 1991.

[87] D. J. Varnes. "Slope movement types and processes". *Special report*, vol. *176*, pp. 11-33, 1978.

[88] D. M. Crudden & D. J. Varnes. "Landslides: investigation and mitigation". Chapter 3-Landslide types and processes. *Transportation research board*, vol. 247, pp. 36-75, 1996.

[89] O. Hungr, S. G. Evans, M. Bovis & J. N. Hutchinson. "Review of the classification of landslides of the flow type": *Environmental and Engineering Geoscience*, vol. 7(3), pp.221-238, 2001.

[90] J. N. Hutchinson. "Morphological and geotechnical parameters of landslides in relation to geology and hydrogeology". In *Proc., Fifth international symposium on landslides, 1988*. Lausanne, AA, vol. 1, pp. 3-35, 1988.

[91] R. M. Iverson. "The physics of debris flows". *Reviews of geophysics*, vol. *35*(3), pp. 245-296, 1997.

[92] T. Takahashi & D. K. Das. "*Debris flow: mechanics, prediction, and countermeasures*." CRC press, vol. 13, pp. 27-77, 2014.

[93] D. Rickenmann. "Empirical relationships for debris flows". *Natural hazards*, vol. *19*, pp. 47-77, 1999.

[94] D. Rickenmann & T. Koch. "Comparison of debris flow modelling approaches". In *Debris-flow hazards mitigation: mechanics, prediction, and assessment*, vol. 1, pp. 576-585. ASCE, 1997.

[95] T. Koch. "Testing of various constitutive equations for debris flow modelling", In: K. Kovar et al. (eds), Hydrology, *Water Resources and Ecology in Headwaters*, vol. 248, pp. 249–257, 1998.

[96] L. Cascini, S. Cuomo & D. Guida. "Typical source areas of May 1998 flow-like mass movements in the Campania region, Southern Italy." *Engineering Geology*, vol. *96*(3-4), pp. 107-125, 2008.

[97] D. D'Ambrosio, S. Di Gregorio, G. Iovine, V. Lupiano, R. Rongo & W. Spataro. "First simulations of the Sarno debris flows through Cellular Automata modelling." *Geomorphology*, vol. *54*(1-2), pp. 91-117, 2003.

[98] L. Capra, J. Lugo-Hubp, & L. Borselli. "Mass movements in tropical volcanic terrains: the case of Teziutlán (México)." *Engineering Geology*, vol. *69*(3-4), pp. 359-379, 2003.

[99] M.T.J. Terlien. "Modelling spatial and temporal variations in rainfall-triggered landslides: the integration of hydrologic models, slope stability models and geographic information systems for the hazard zonation of rainfall-triggered landslides with examples from Manizales (Colombia)." *International Institute for Aerial Survey and Earth Sciences* (ITC), pp. 9-39, 1996.

[100] G. B. Chirico. “Hydrologic conditions leading to debris-flow initiation in the Campanian volcanoclastic soils”. *Mediterranean Storms*, vol. 1, pp. 473-484, 2000.

[101] F.M. Guadagno, P.A.L.A. Revellino & G. Grelle. “The 1998 Sarno landslides: conflicting interpretations of a natural event.” In *International conference on debris-flow hazards mitigation: mechanics, prediction, and assessment, proceedings* pp. 71-81, 2011.

[102] M.T. Pareschi, R. Santacroce, R. Sulpizio & G. Zanchetta. “Volcaniclastic debris flows in the Clanio Valley (Campania, Italy): insights for the assessment of hazard potential.” *Geomorphology*, vol. *43*(3-4), pp. 219-231, 2002.

[103] M. Arattano, G. Bertoldi, M. Cavalli, F. Comiti, V. D’Agostino & J. Theule. “Comparison of methods and procedures for debris-flow volume estimation”. In *Engineering Geology for Society and Territory-Volume 3: River Basins, Reservoir Sedimentation and Water Resources* pp. 115-119. Springer International Publishing, 2015.

[104] C. Scheild & D. Rickenmann. “Top Flow DF-a simple GIS based model to simulate debris-flow runout on the fan”. *Italian journal of engineering geology and environment*, vol. 1, pp. 253-262, 2011.

[105] M. S. Adams, R. Fromm & V. Lechner. “High-resolution debris flow volume mapping with unmanned aerial systems (UAS) and photogrammetric techniques”. The International Archives of the Photogrammetry, Remote Sensing and Spatial Information Sciences, vol. 41, pp. 749-755, 2016.

[106] D. O. Dorta, G. Toyos, C. Oppenheimer, M.T. Pareschi, R. Sulpizio & G. Zanchetta. “Empirical modelling of the May 1998 small debris flows in Sarno (Italy) using LAHARZ”. *Natural Hazards*, vol. *40*, pp. 381-396, 2007.

[107] O. Hungr, G.C. Morgan & R. Kellerhals. “Quantitative analysis of debris torrent hazards for design of remedial measures”. *Canadian Geotechnical Journal*, vol. *21*(4), pp. 663-677, 1984.

[108] T. Mizuyama, S. Kobashi & G. Ou, G. “Prediction of debris flow peak discharge”. In *Internationales symposion: Interpraevent*, pp. 99-108, 1992.

[109] M. A. Rahman. “Ascertaining a hands-on approach to estimate debris flow velocities for rational debris hazard mitigation”. *PhD Diss. Civil Engineering, Yokohama Natl Univ, Yoklahama, United States, 2016.*

[110] K. Hu, M. Tian & Y. Li. “Influence of flow width on mean velocity of debris flows in wide open channel”. *Journal of Hydraulic Engineering*, vol. *139*(1), pp. 65-69, 2013.

[111] S. P. Pudasaini & S. A. Miller. “A real two-phase submarine debris flow and tsunami”. In *AIP Conference Proceedings* Vol. 1479, No. 1, pp. 197-200. American Institute of Physics, 2012.

[112] T. Takahashi. Debris flow. *IAHR, Monograph Series, 1991*.

[113] S. Guo, P. Xu, Z. Zheng & Y. Gao. “Estimation of flow velocity for a debris flow via the two-phase fluid model”. *Nonlinear Processes in Geophysics*, vol. *22*(1), pp. 109-116, 2015.

[114] D. D'Ambrosio, S. Di Gregorio, G. Iovine, V. Lupiano, R. Rongo & W. Spataro. “First simulations of the Sarno debris flows through Cellular Automata modelling.” *Geomorphology*, vol. *54*(1-2), pp. 91-117, 2003.

[115] M. H. Bulmer, O. S. Barnouin-Jha, M. N. Peitersen & M. Bourke. “An empirical approach to studying debris flows: Implications for planetary modelling studies”. *Journal of Geophysical Research: Planets*, vol. *107*(E5), p. 9, 2002.

[116] A. B. Prochaska, P. M. Santi, J. D. Higgins & S. H. Cannon. “A study of methods to estimate debris flow velocity”. *Landslides,* vol. *5*, pp. 431-444, 2008.

[117] T. C. Pierson. “Flow characteristics of large eruption-triggered debris flows at snow-clad volcanoes: constraints for debris-flow models”. *Journal of volcanology and geothermal research*, vol. *66*(1-4), pp. 283-294,1995.

[118] K. J. Hsu. “Catastrophic debris streams (sturzstroms) generated by rockfalls”. *Geological Society of America Bulletin*, vol. *86*(1), pp. 129-140, 1975.

[119] G. Toyos, R. Gunasekera, G. Zanchetta, C. Oppenheimer, R. Sulpizio, M. Favalli & M.T. Pareschi. “GIS-assisted modelling for debris flow hazard assessment based on the events of May 1998 in the area of Sarno, Southern Italy: II. Velocity and dynamic pressure”. *Earth Surface Processes and Landforms: The Journal of the British Geomorphological Research Group*, vol. *33*(11), pp. 1693-1708, 2008.

[120] G. P. Toyos, P. D. Cole, A. Felpeto & J. Marti. “A GIS-based methodology for hazard mapping of small volume pyroclastic density currents”. *Natural Hazards*, vol. *41*, pp. 99-112, 2007.

[121] S. P. Schilling. Laharz_py: “GIS Tools for Automated Mapping of Lahar Inundation Hazard Zones”; Open-File Report 2014-1073. *US Geological Survey: Reston, VA, USA, 2014.*

[122] R. M. Iverson, S. P. Schilling & J. W. Vallance. “Objective delineation of lahar-inundation hazard zones”. *Geological Society of America Bulletin*, vol. *110*(8), pp. 972-984, 1998.

[123] C. S. Magirl, P. G. Griffiths & R. H. Webb. “Analyzing debris flows with the statistically calibrated empirical model LAHARZ in southeastern Arizona, USA. *Geomorphology*, vol. *119*(1-2), pp. 111-124, 2010.

[124] J. P. Griswold & R.M. Iverson. *Mobility statistics and automated hazard mapping for debris flows and rock avalanches*. US Department of the Interior, US Geological Survey, 2008.

[125] https://rischi.protezionecivile.gov.it/en/approfondimento/national-dataset-of-italian-structural-aggregates/

[126] M.T. Pareschi, M. Favalli, F. Giannini, R. Sulpizio, G. Zanchetta & R. Santacroce. “May 5, 1998, debris flows in circum-Vesuvian areas (southern Italy)”: Insights for hazard assessment. *Geology*, vol. *28*(7), pp. 639-642, 2000.

[127] G. Zanchetta, R. Sulpizio, M.T. Pareschi, F.M. Leoni, & R. Santacroce. “Characteristics of May 5–6, 1998 volcaniclastic debris flows in the Sarno area (Campania, southern Italy): relationships to structural damage and hazard zonation”. *Journal of volcanology and geothermal research*, vol. *133*(1-4), pp. 377-393, 2004.

[128] G. Toyos, C. Oppenheimer, M.T. Pareschi, R. Sulpizio, G. Zanchetta & G. Zuccaro. “Building damage by debris flows in the Sarno area, Southern Italy”. In *Proceed. Third international conference on debris-flow hazards mitigation: mechanics, prediction and assessment* Vol. 2, pp. 1209-1220, 2003.

VITA

Fidence Cyizere Rukundo received his B.Sc. degree in Civil Engineering from Kocaeli University in June 2021. Since September 2021, he has been working on his M.Sc. in Civil Engineering at Özyeğin University under the supervision of Dr. Derya Deniz (Advisor) and Dr. Yiğit Can Altan (Co-Advisor).